NCU-T-78-010 c. 2

Working Paper 78-1

DETERIORATION OF ASBESTOS CEMENT SHEET MATERIAL IN THE MARINE ENVIRONMENT

LOAN COPY ONLY

J. Machemehl
L. Watson
B. Barnes

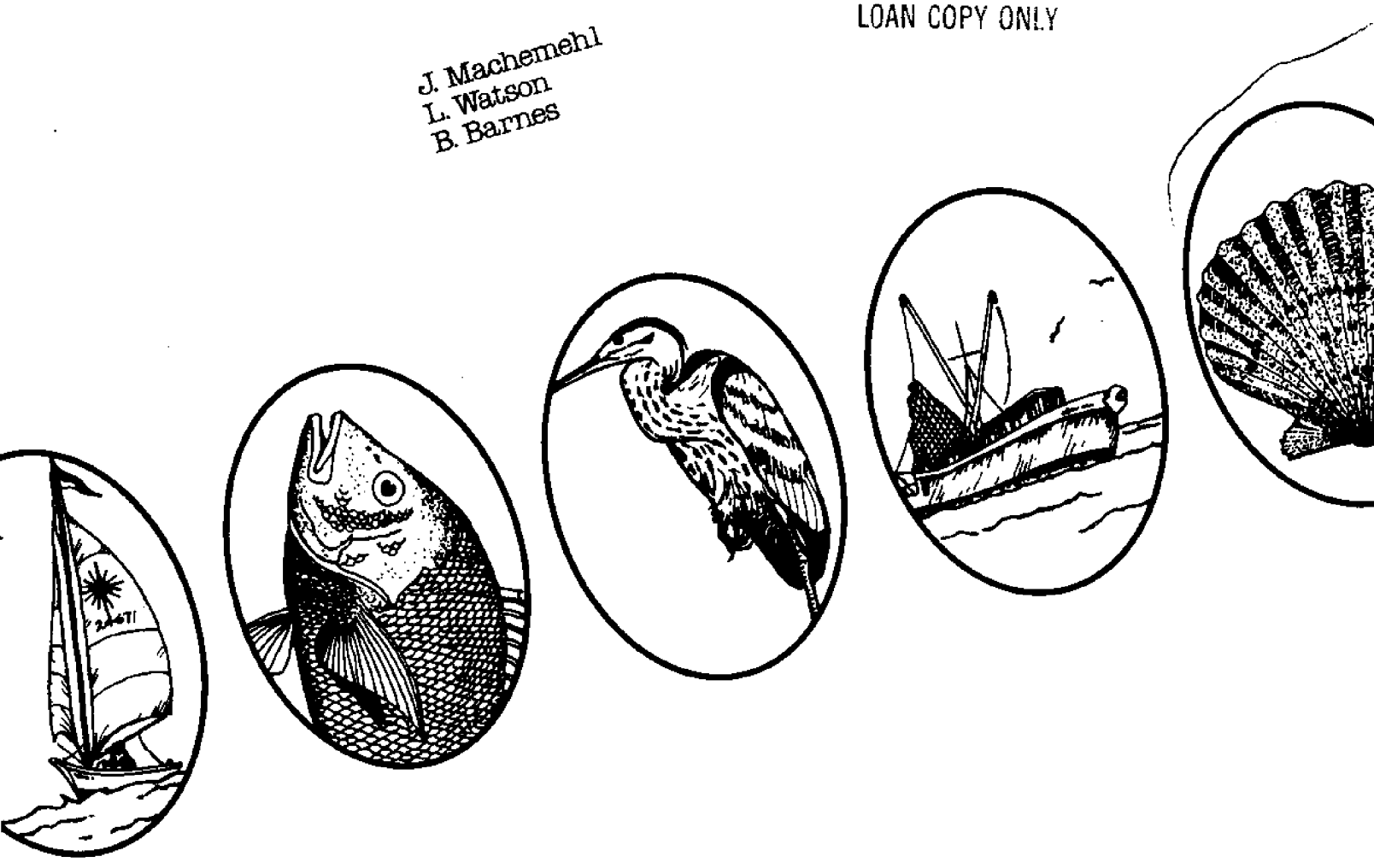

UNC Sea Grant College Program
105 1911 Building
North Carolina State University
Raleigh, NC 27650

DETERIORATION OF ASBESTOS CEMENT SHEET MATERIAL IN THE MARINE ENVIRONMENT

LOAN COPY ONLY

by

Jerry L. Machemehl
Department of Marine Science and Engineering

and

Larry E. Watson and Bobby D. Barnes
Department of Civil Engineering
North Carolina State University
Raleigh, North Carolina 27650

This work was partly sponsored by the Department of Marine Science and Engineering and the Office of Sea Grant, NOAA, U.S. Department of Commerce, under Grant No. 04-8-M01-16 and the North Carolina Department of Administration. The U.S. Government is authorized to produce and distribute reprints for governmental purposes not withstanding any copyright that may appear hereon.

Department of Marine Science
and Engineering Publication No. 78-6

UNC Sea Grant College
Working Paper 78-1

December, 1978

NATIONAL SEA GRANT DEPOSITORY

ABSTRACT

Tests were conducted on asbestos cement sheet piling to determine the causes of corrosion to the material along the North Carolina coast. New sheets of asbestos cement were obtained from which 78 specimens were fabricated. A wetting/drying apparatus was used to simulate tidal conditions. Three months of wetting/drying were carried out with both fresh water and seawater. Asbestos cement samples were removed at the end of each month and tested for tensile strength. Selected samples were then examined with the aid of the x-ray diffractometer and scanning electron microscope for determination of material composition.

A study of an asbestos cement bulkhead from the field was also conducted. Samples were tested for tensile strength, then analyzed with the diffractometer and scanning electron microscope. The asbestos cement bulkhead under investigation from the field was severely deteriorated through the reaction of aggressive CO_2 with $CaCO_3$ in the material. The $Ca(HCO_3)_2$ which was formed was leached out of the structure in solution, thus causing a drop in material density and increase in porosity. Asbestos cement bulkheads were found vulnerable to carbonic acid attack in canals and estuaries where biological decay produced an excess of dissolved CO_2 and the water's pH was less than 7. Autoclaved asbestos cement delayed the extensive deterioration due to carbonic acid. It contains a high amount of silica which was non-reactive at normal temperatures. Autoclaved asbestos cement was however subject to corrosion in seawater. The cause of this corrosion is debatable, but it is likely that the presence of a sulphate concentration along with the wetting/drying process invoked by tidal action plays a major role in the mechanism of deterioration.

ACKNOWLEDGEMENTS

The authors wish to express their appreciation to the Department of Marine Science and Engineering and the Office of Sea Grant, NOAA, U.S. Department of Commerce for supporting the research.

TABLE OF CONTENTS

TABLE OF CONTENTS (Continued)

LIST OF TABLES

LIST OF FIGURES

LIST OF FIGURES (continued)

INTRODUCTION

Asbestos cement sheets have become a popular construction material for bulkheads (see Table 1.) in coastal areas such as sounds and canals which are subjected to wave action.

Table 1. Asbestos Cement Sheet Pile Bulkheads in North Carolina.

Year	Asbestos Cement Sheet Pile Bulkheads Constructed in North Carolina*	
	Linear Meters	Linear Feet
1973	6,019	19,743
1974	5,092	16,700
1975	619	2,029
1976	2,414	7,918
1977	1,422	4,665

* Information obtained from Permit Applications, Division of Commercial and Sports Fisheries, State of North Carolina.

These bulkheads are often exposed to tidal fluctuations which give rise to a wetting and drying phenomena. Due to the short length of time that asbestos cement has been utilized at the coast, very little (if any) research has been conducted as to the effect of seawater on this construction material.

Recently, severe deterioration has occurred in asbestos cement bulkheads located in the coastal zone of North Carolina. The purpose of this investigation is to examine asbestos cement material used in bulkhead construction through laboratory simulation of

deterioration mechanisms common to coastal regions of North Carolina. A field sample from a deteriorating bulkhead is also examined. The different causes of asbestos cement corrosion based upon previous research concerned with destructive processes on Portland cement are discussed.

LITERATURE REVIEW

The Hydration and Hydration Products of Portland Cement

Portland cement is commercially available for a wide range of uses. The composition of Portland cement in the United States is controlled by ASTM Specification C150 and varies within four cement types. All of these cements may be characterized chemically by the oxides, CaO, Sio_2, Al_2O_3, and Fe_2O_3. Type I, ordinary Portland cement, is widely used where no special design limitations control. Type II, modified Portland cement, has restrictions placed on the amount of Al_2O_3 and Fe_2O_3 in the composition and is a general purpose, moderately sulphate-resisting cement. Type III, rapid-hardening Portland cement, is basically the same as Type I except that the mixture is usually more finely ground. Type III allows more surface area for cement-water interaction, and thus a faster rate of hydration. Type V, sulphate-resisting Portland cement, is similar to Type II but has a more severe limitation placed on the Al_2O_3 and Fe_2O_3 contents. Type V cement is used where severe environmental conditions exist.

Portland cement is manufactured by burning raw materials such as clay, limestone, and sand along with the addition of minor constituents to form a clinker. The ground clinker is composed of the cementing agents, tricalcium silicate (C_3S), dicalcium silicate (C_2S), tricalcium aluminate (C_3A), and tetracalcium aluminoferrite (C_4AF).[1] C_3S may be considered to provide most

---

[1] The following notations are standard for identifying the clinker constituents: CaO=C, Sio_2=S, Al_2O_3=A, Fe_2O_3=F. A subscript after one of these symbols indicates multiplicity of the oxide, i.e., $3CaO \cdot Sio_2 = C_3S$, etc.

of the characteristic strength of Portland cement with C_2S being a by-product of the burning process (Biczok, 1967; Czernin, 1962 and Lea, 1970). The addition of both alumina and ferric oxides has been found to enhance the formation of C_3S during the burning process, and, as a result, C_3A and C_4AF are formed (Hadley, 1970).

The addition of water to Portland cement initiates hydration of the clinker constiuents. The main cementing product formed through this hydration is known as calcium silicate hydrate (CSH) gel. This compound is sometimes referred to as tobermorite due to its resemblance to the naturally occurring mineral tobermorite and is found in several different forms in hardened cement (Lea, 1970). A by-product of the formation of CSH gel is calcium hydroxide, which is involved in weathering processes of hardened cement. The other hydrates of importance formed during the hydration process include the calcium aluminate hydrates, specifically those formed through the hydration of C_3A. These are especially important when determining the proportions of additives that should be included in the cement mix and the resistance of the hardened cement to a sulphate-rich environment.

The primary additive controlled by the C_3A content is gypsum ($CaSO_4 \cdot 2H_2O$). When added to the clinker, gypsum reacts with C_3A, retarding hydration through the formation of a calcium sulphoaluminate. This reaction results in either a low-sulphate form or a high-sulphate form known as ettringite, a very expansive, insoluble compound. Although the formation of ettringite is helpful for structural stability in the early stages of hydration, its expansive nature can cause destruction of the cement when formed after

the hydration process has been completed. Other additives commonly used are silica, important in autoclaved Portland cement, and pozzolans, believed by many researchers to enhance the resistance of Portland cements to harsh environments (Atwood and Johnson, 1924; Biczok, 1967; Czernin, 1962; Lea, 1970 and Wakeman, et al., 1958).

Autoclaved Portland Cement

Many precast cement products are manufactured by a high-pressure, steam-curing process known as autoclaving. Curing cement in an autoclave results in high early strength, sometimes greater than that obtained at 28 days under normal curing (Lea, 1970). The process consists of an initial moist curing period after which the cement is subjected to a combined steam-pressure cure. The pressure applied and the length of the curing period are dependent upon the required strength of the cement and the mineral content of the cement.

Silica, usually in the form of quartz, is the most common addition to Portland cement that is to be cured in an autoclave. Under normal curing conditions, silica does not react with the cement particles, but combines with the cementing compounds mechanically (Lea, 1970). However, during autoclaving the silica and free lime (occurring as $Ca(OH)_2$) react to provide strength and less permeability to the finished product in the form of CSH gel. This reaction allows the autoclaved cement to be more durable to the effects of weathering and sulphates.

The Manufacture of Asbestos Cement

The production of asbestos cement products is unique ,differing

from that of typical concrete and cement products. The main components of asbestos cement are the fibrous serpentine, chrysotile, and Portland cement. The chrysotile fibers are mixed with cement in a slurry to form the cement matrix. This slurry then passes onto a revolving cylinder for deposition onto a continuous felt sheet. The excess water is then removed in the production process. A smooth, metal molding cylinder picks up the coated fibers from the felt in a thin layer and rotates until the desired sheet thickness is obtained. The roll is then cut open and laid out in a sheet from which a corrugated shape may be molded. A more detailed account of this procedure is presented by the U.S. Bureau of Mines (Bowles, 1937).

Asbestos cement products which are cured in an autoclave are usually formed by the use of a dry mix process. The same components as mentioned above, along with silica flour, are mixed, then passed onto a conveyor belt where hot water is sprayed on the mix. This product is then consolidated by rollers and cured in an autoclave (Bowles, 1937).

The asbestos cement products studied herein were composed of Type II Portland cement. The hydration products then are those that are produced by the use of this cement. These products in the processes mentioned above are the same as would be expected from the hydration of normally cured and autoclaved Portland cement as previously reported (Kalousek, et. al., 1966). One property of asbestos cement products is the high tensile strength, resulting from the presence of the asbestos fibers. This allows for the manufacture of a thinner material than most other cement products.

Seawater and Cement

Many field and laboratory studies have been conducted on concrete structures in marine environments (Atwood and Johnson, 1934; Biczok, 1967; Lea, 1970; Terzaghi, 1948 and Wakeman, et. al., 1958). Also, much research has been done to determine the mechanisms through which seawater attacks cement. Findings have shown that concrete corrosion in seawater can be caused by high sulphate concentrations, excessive CO_2 in the water (carbonation), dissolving of readily soluble compounds produced by ion exchange, and the effects of freezing and thawing action on the material (Biczok, 1967 and Lea, 1970). Often, the deterioration is likely to be a combination of these modes of corrosion rather than the effect of a single mode.

Field studies of in-place concrete have been reviewed by Wakeman, et al. (1958). One of the earliest studies was conducted by Hughes in 1905 as reported by Mehta and Haynes (1975). This experiment consisted of the placement of 16 concrete blocks in the Los Angeles Harbor. After 27 years of exposure to the seawater, the blocks were removed and studied for deterioration. The tests indicated that magnesia had replaced some of the lime of the cement. Otherwise, the material was found to be free from corrosion. The blocks were returned to the harbor and, after 67 years of exposure six were removed a second time by Mehta and Haynes (1975). The data obtained in this study indicated an attack by seawater. It was determined that both sulphate attack by the formation of gypsum from the lime of the cement and acid attack by carbonation were the modes of deterioration of the concrete. The most notable corrosion occurred in the least dense concrete.

Terzaghi (1948) noted similar deterioration in an investigation of a shipway at Newport News, Virginia. The shipway concrete was composed of both Type I and Type II Portland cement, with the most extensive corrosion occurring in those sections with the Type I cement. Terzaghi concluded that the expansion and cracking found were due to sulphate attack of the gypsum/ettringite type, while the sections which incurred a loss of strength were deteriorated by carbonation of the free lime in the concrete. The portions of the shipway subjected to carbonation showed disintegration as well as surface softening due to the chemical process.

Numerous studies (Atwood and Johnson, 1924; Biczok, 1967 and Lea, 1970) report in detail the probable mechanisms of corrosion of concrete in contact with seawater . The three most common destructive agents pertaining to seawater - sulphate attack, high CO_2 content, and freezing and thawing actions-will be examined.

As previously indicated, gypsum can react with C_3A to form ettringite. In the case of hydrated cement, this reaction occurs only if there is unreacted C_3A and gypsum is present. The $Ca(OH)_2$ which is the hydration product of normally cured Portland cement is capable of reacting with the sulphates present in seawater to form gypsum through the reaction:

$$Ca(OH)_2 + SO_4^{-2} + 2H_2O = CaSO_4 \cdot 2H_2O + 2(OH)^- \quad \text{.....(1)}$$

This result alters the hydration of C_3A as the calcium sulphate solution penetrates into the cement causing rapid expansion through the formation of ettringite:

$$C_3A + 3CaSO_4 + 31H_2O = C_3A \cdot 3CaSO_4 \cdot 31H_2O \quad \text{.....(2)}$$

The expansion produced in this reaction, which is on the order of 36% volume change, leads to extensive internal swelling and eventually cracking of the cement. This form of deterioration is considered the major cause of concrete corrosion in seawater (Lea, 1970).

Even when the C_3A content is low, however, expansive deterioration can occur if there is a significant amount of $Ca(OH)_2$ to react in the formation of gypsum as previously mentioned. Although volume expansion due to gypsum formation is only around 12%, it can be just as destructive as ettringite when formed in high sulphate conditions (Biczok, 1967). Gypsum in seawater is very soluble. It can dissolve upon formation and wash away, causing deterioration of the cement face exposed to seawater (Biczok, 1967 and Lea, 1970).

There is some disagreement concerning the amount of sulphate present in solution above which the solution becomes aggressive to cement. Biczok (1967) lists the sulphate limitations specified by the codes of different countries. The recommended limits for sulphate aggressivity in the U.S. as established by the ACI are given in Table 2 along with the recommended cement type (Committee 201 Report, 1977).

The action of cyclic freezing and thawing is very destructive to low density, permeable cement products such as asbestos cement. This phenomenon is common in cold regions where temperature varies drastically and frequently between $0^{\circ}F$ and $40^{\circ}F$. Cement products in coastal areas which have severe winters are subject to freezing and thawing as a result of tidal fluctuations which saturate the

Table 2. Limits of SO_4 to Avoid Attack on Concrete by Sulphates as Specified by the ACI.

Degree of Attack	Water Soluble Sulphate (SO_4), %	Sulphate (SO_4) in Water, ppm	Cement Type Recommended
Mild	0.00-0.10	0-150	———
Moderate	0.10-0.20	150-1500	Type II
Severe	0.20-2.00	1500-10,000	Type V
Very Severe	Over 2.00	Over 10,000	Type V + Pozzolan

cement and then leave it exposed to the weather (Biczok, 1967). There is disagreement among investigators as to whether the mechanism of destruction is the formation of ice crystals or the pressure exerted internally by the crystals forming in the capillaries of the cement paste (Lea, 1970). A detailed description of cement freezing and thawing is presented by Arni (1972). Examples of deterioration due to freezing and thawing can also be found in the literature (Idorn 1964 and Kennedy and Mather 1954).

The last corrosive agent common to seawater that will be discussed is the presence of excessive CO_2 dissolved in the water. Carbon dioxide is absorbed from the air by bodies of water and is formed in high concentrations in waters where organic decay is common such as in estuaries and bays. Corrosion occurs when the dissolved CO_2 combines with the hydrogen ion in large enough quantity to cause a carbonic acid (H_2CO_3) attack on the cement. Although this mode of destruction is not generally considered serious, the scope of this study warrants a close investigation into the deterioration mechanisms of carbonic acid attack.

The Effect of Carbon Dioxide on Cement

Carbon dioxide can react with hydrated Portland cement either through the atmosphere or through solution in its dissolved state, H_2CO_3. Almost all normally cured cement products exposed to the environment will react with CO_2 through the cement's free $Ca(OH)_2$ content to form $CaCO_3$.

$$Ca(OH)_2 + CO_2 = CaCO_3 + H_2O \quad (3)$$

The extent to which this reaction takes place is dependent on the thickness of the cement material, its density, and the free $Ca(OH)_2$ available. While the formation of $CaCO_3$ due to atmospheric carbonation enhances the strength and stability of cement paste, the effect of carbonic acid is very detrimental to cement.

One of the primary factors in the destructiveness of carbonic acid attack is the amount of aggressive CO_2 found in solution of the water. Aggressive CO_2 is that CO_2 which is free to attack $CaCO_3$ in the following reaction:

$CaCO_3 + H_2CO_3 = Ca(HCO_3)_2$ .....(4)

However, both H_2CO_3 and $Ca(HCO_3)_2$ react with $Ca(OH)_2$ to form $CaCO_3$.

$Ca(OH)_2 + H_2CO_3 = CaCO_3 + 2H_2O$ .....(5)

$Ca(OH)_2 + Ca(HCO_3)_2 = 2CaCO_3 + 2H_2O$ .....(6)

Calcium bicarbonate is a very unstable compound which decomposes to form $CaCO_3$ if sufficient H_2CO_3 is not present to stabilize the compount. If more H_2CO_3 is available than is required to stabilize $Ca(HCO_3)_2$, then $CaCO_3$ is attacked by the carbonic acid. A graphical method for determining the amount of aggressive carbonic acid available in a given water sample is discussed by Terzaghi (1949) and Lea (1970). This procedure is dependent on knowledge of the free CO_2 content as well as the amount of CO_2 contained in $Ca(HCO_3)_2$.

Carbonic acid corrosion takes place in cement through percolation. Successive stages of this corrosion, schematically represented in Figure 1, are reported by Biczok (1967). There are three mechanisms by which carbonic acid alters the makeup of cement as the water seeps through the structure. They are represented in Figure 1 as zones of (a) deterioration, (b) strength gain, and (c) leaching.

The deterioration zone is characterized by the formation of $Ca(HCO_3)_2$ through the reaction between H_2CO_3 and $CaCO_3$. Most cement products form an outer layer of $CaCO_3$ by exposure to the atmospheric CO_2 prior to structural application. If the structure is located in an environment containing aggressive CO_2, all of the $Ca(OH)_2$ is depleted from the surface layer, leaving the cement open to attack by $CaCO_3$ dissolving in the form of $Ca(HCO_3)_2$.

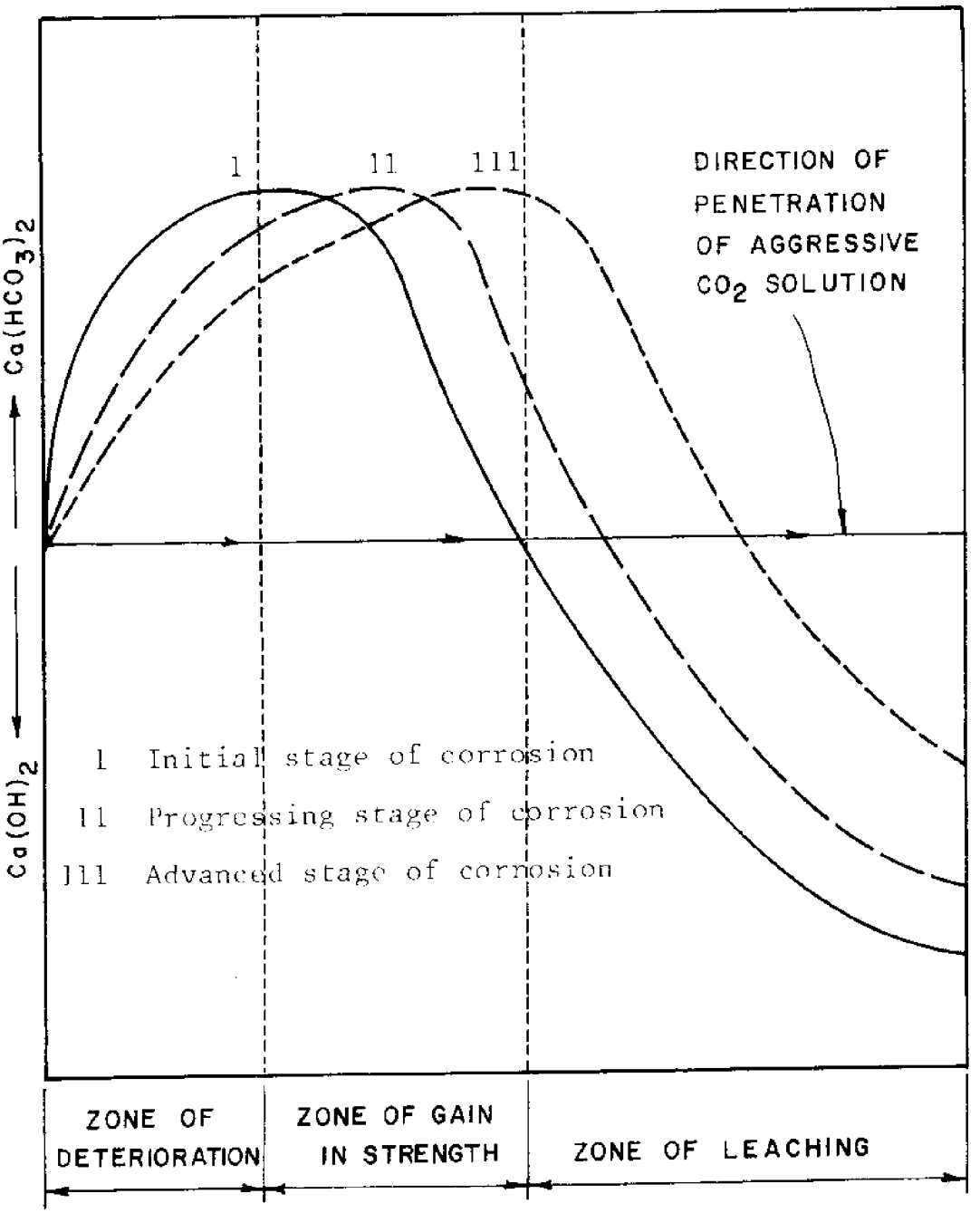

Figure 1. Stages of Corrosion Due to Carbonic Acid Attack. (After Biczok, p. 285 (1967)).

The bicarbonate-saturated water penetrates the structure, and uncarbonated water is therefore vulnerable to the aggressive CO_2 as well as the $Ca(HCO_3)_2$ in solution. The effect is initially beneficial, since $CaCO_3$, which is poorly soluble, is precipitated by both reactions. The dense nature of $CaCO_3$ leads to a strengthening of the material, hence the name of the second zone of cement transformation.

After enough $Ca(OH)_2$ has reacted with the percolating water to deplete the solution of its aggressive CO_2, removal of the other cementing constituents takes place through the physical movement of the water. This leaching zone leads to a seepage flow which is evidence of how far advanced the deterioration of the cement is. If bicarbonate is found in the flow, the cement is highly corroded, and deterioration can be expected to increase.

Field evidence of carbonic acid attack has been discussed, Metha and Haynes (1975) and Terzaghi (1948). Numerous other studies have also attested to the significance of this form of cement deterioration (Cole and Kroone, 1960; Powers, 1962; Sauman, 1971; Shideler, 1963; Verbeck, 1958). The findings indicate, among other things, a correlation between pH of a solution and aggressivity of H_2CO_3, a measure of strength of the cement as a function of $Ca(OH)_2$ remaining, and an interesting series of transformations of $CaCO_3$ through carbonation.

The effect of the pH of a solution on the corrosion of cement due to carbonic acid is discussed at length by both Lea (1970) and Biczok (1967). It has been found that waters of aggressive CO_2 with a pH above 7 (i.e. alkaline) have very little detrimental effect on cement. Whereas, similar waters with a pH

below 7 (i.e. acidic) were found to be very destructive to cement. Sverdrup, et al. (1948) have determined the pH of the open ocean to range from 8.0 to 8.2, in which case seawater would not be considered aggressive in conjunction with carbonic acid. However, Terzaghi (1949) points out that in sheltered bays and estuaries this pH value can drop to 7 or less, allowing possible attack of the cement by carbonation. She substantiates this position with the findings in her study at Newport News, Virginia.

Tremper (1931) investigated the effects of carbonation on the strength of concrete. He concluded that the loss of CaO from the cement caused a decrease in strength at a rate of 1:2. With the loss of half of the original lime content in a cement structure, full loss of strength is attained. Tremper also concluded that structures with a high surface/volume ratio are subject to an increased rate of attack.

Cole and Kroone (1960), in a study of Portland cement paste, report that after carbonation of normally cured and autoclaved samples almost no $Ca(OH)_2$ could be detected through x-ray diffraction analysis. A further examination of the analysis revealed that $CaCO_3$ was present in the three forms of calcite, vaterite, and aragonite. In both normally cured and autoclaved samples, calcite was predominant over vaterite and aragonite. However, in the normally cured samples vaterite predominated over aragonite, while in the autoclaved samples the opposite was true.

Sauman (1971) found $CaCO_3$ present in these same three forms when he studied the carbonation of autoclaved, porous concrete and calcium silicate hydrate (CSH) gel (the binding constituent

found in asbestos cement, (Kalousek, et. al., 1966). He concluded that vaterite and aragonite were formed in amounts dependent upon humidity and CO_2 concentration. These then transform, with age, into calcite, which is a more stable phase of $CaCO_3$. Also, the autoclaved, porous concrete, which contained 67% quartz by weight, showed a strong diffraction pattern of silica upon carbonation.

RESEARCH APPARATUS AND PROCEDURES

Wetting/Drying Apparatus

Three months of accelerated tests were performed in a wetting/drying apparatus (see Figure 2). This assembly consisted of two tanks 40.6 cm x 40.6 cm x 244 cm (1.33 ft. x 1.33 ft. x 8.0 ft.). The tanks were lined with a plastic sheet for water retention, with one tank holding sea water and the other holding fresh water. Mounted over the tanks was a rotating assembly which held the test samples. Driving this assembly was a 1/4 H.P., bidirectional, D.C. gear motor which had a maximum output of 17 R.P.M. The motor was geared down to approximately 5 R.P.M. for use in this test by varying the voltage with a voltage regulator. A series of 16, 250-watt heat lamps were placed approximately 46 cm (1.51 ft.) from the center of the tanks along the length of the assembly. A 24 hr. timer along with microswitches attached to the end of the assembly controlled the off/on sequence of the lamps and motor and allowed for continuous cycling.

Hydraulic Testing Machine

The test samples were pulled to failure for tensile strength comparison. These tests were conducted with a 266,800 N (60,000 lb.) capacity Southwark hydraulic testing machine on the 0-266,800 N (0-6000 lb.) scale. Samples were held in place by two stocks containing grip-type clamps and were loaded at a rate of about 133.4 N/sec. (30 lbs./sec.).

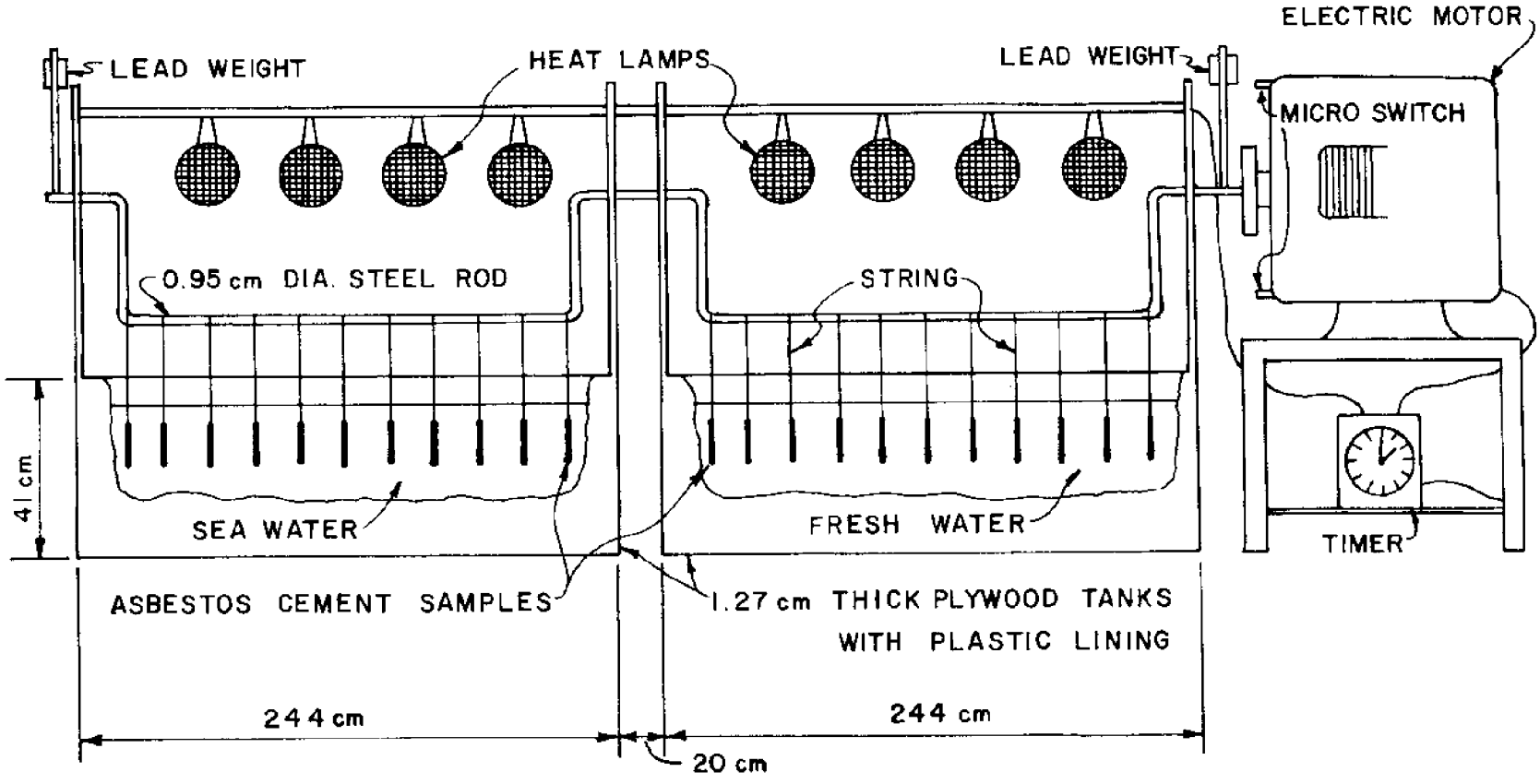

Figure 2. Schematic Representation of Wetting/Drying Apparatus.

(Note: Wetting Cycle)

X-Ray Diffractometer

X-ray Diffraction patterns were obtained through the use of a North American Philips, Norelco X-ray Diffractometer. The diffractometer was equipped with a copper element and nickel filter and was operated at 35 kv./20 ma. Diffraction peaks were recorded on graph paper at 2θ degrees at a rate of 1 ^{o}/min. The recorder was set at a scale factor of 2 and a time constant of 2 sec. for the series of tests.

Scanning Electron Microscope

A Jelco, JSM-II Scanning Electron Microscope (SEM) was used to identify the crystalline components of the system from their morphology as contained in the specimens as well as to identify the compounds through their elemental components. An accessory to the SEM was an EDAX model 707A which enabled the use of an energy dispersive analysis of x-rays in determining the elements common to the specimen material.

New Asbestos Cement Sheets

Sample Preparation. Six new asbestos cement sheets were purchased for use in the laboratory tests. These sheets were 1.22 m (4.0 ft.) wide and 1.83 m (6.0 ft.) long with a 0.95 cm (0.375 in.) thickness. The material had been pressed into a corrugated shape and cured in an autoclave. This asbestos cement was composed of chrysotile fibers and Type II Portland cement with silica added to combine with the free lime upon autoclaving.

Determination of the shape of the samples desired for the tests was based upon the limitations of the wetting/drying apparatus as well as the Southwark loading machine. Overall dimensions of the specimens were 5 cm x 19.7 cm (2 in. x 7 3/4 in.) with a mid-section tapered to 2.5 cm (1 in.) to allow for over-stressing due to material inconsistencies (see Figure 3).

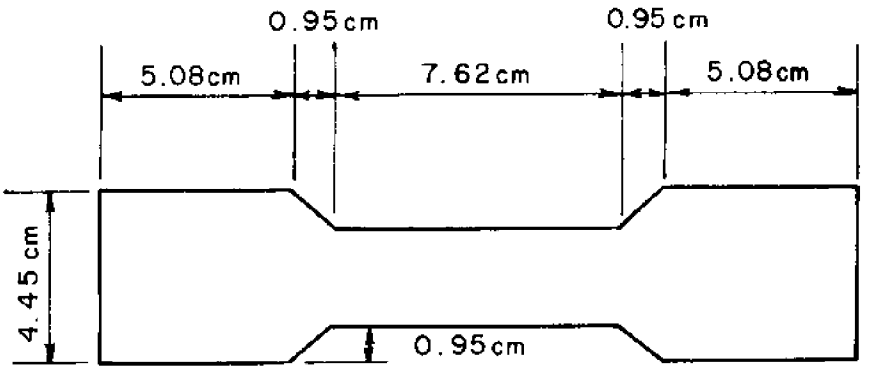

Figure 3. Typical Sample Dimensions

Pilot Test. Four samples were fabricated from each of the six asbestos cement sheets for use in a pilot test (1) to establish the length of the wetting and drying cycles and (2) to determining the number of samples needed to obtain statistically valid results in the test program.

Two of the four specimens from each sheet were weighed then placed in a tank filled with fresh water and allowed to soak, while the remaining specimens were kept as control samples. The soaked samples were removed and weighed at 15 min. intervals with the surface dry, until little or no change in weight occurred between the intervals. The time to saturation was approximately one hour, with about 95% of saturation occurring after 45 min. as shown in Table 3.

Once the samples had become saturated, they were placed in an oven at $95^{o}C \pm 5^{o}C$. Again, the specimens were removed every 15 min. and weighed, this time until their original dry weight was obtained. As with the soaking cycle, drying to the original weight was approximately achieved in one hour as shown in Table 4.

After the wetting and drying cycles had been established, the specimens were subjected to a total of twenty cycles from the dry state through saturation, then back to dry. Upon completion the twelve wet and dried samples along with twelve remaining samples were loaded to failure in tension. Their maximum stresses were recorded in Tables 9 and 10 in Appendix A. Average stresses were calculated for statistical evaluation.[2]

---

[2] One value was omitted when the machine was reloaded before the stress value had been recorded.

Table 3. Preliminary Test: Saturation Study.

Time	Samples (% of saturation)					
	1-A	1-B	2-A	2-B	3-A	3-B
10:30	0	0	0	0	0	0
10:45	77.6	75.6	76.0	75.0	65.0	65.4
11:00	94.1	86.6	88.0	86.9	76.7	77.1
11:15	96.5	98.8	97.0	96.8	88.3	88.2
11:30	100	100	98.8	98.8	95.1	94.8
11:45	100	100	100	100	100	100
14:00	100	100	100	100	100	100
	4-A	4-B	5-A	5-B	6-A	6-B
10:30	0	0	0	0	0	0
10:45	75.3	75.5	74.5	76.7	77.4	80.4
11:00	89.2	89.6	88.2	89.6	89.9	92.6
11:15	96.4	98.8	98.0	98.2	99.4	99.4
11:30	100	100	99.3	100	100	100
11:45	100	100	100	100	100	100
14:00	100	100	100	100	100	100

Table 4. Preliminary Test: Drying Phase (Oven).

Time	Samples (% of saturation)					
	1-A	1-B	2-A	2-B	3-A	3-B
16:00	100	100	100	100	100	100
16:15	47.1	49.4	52.7	55.6	60.7	60.8
16:30	30.6	28.7	34.1	36.3	44.2	43.1
16:45	14.7	13.4	16.2	18.8	27.0	27.5
17:00	0	1.2	0.6	1.3	2.3	2.4
	4-A	4-B	6-A	5-B	6-A	6-B
16:00	100	100	100	100	100	100
16:15	57.8	56.4	53.6	49.7	50.3	54.6
16:30	39.2	38.0	34.0	30.1	31.4	35.6
16:45	28.9	20.9	15.7	13.5	12.6	18.4
17:00	2.3	1.3	0	-3.7	-5.0	0.6

The procedure used for determining the sampling size for the test program was a standard probabilistic technique with a t-distribution (Waldole and Myers, 1972). The number of samples needed was a function of the accuracy required, the standard deviation of the stresses obtained, and a confidence interval for the maximum stresses. To be 95% confident that the mean stress obtained would fall within a range of 190 N/cm (0.045 lb./ft.^{2}), the sample size was determined to be twelve for the wet and dried samples and three for the control samples. Details are provided in Appendix B.

Test Program. The test program was based upon the sampling size, the specimens' shape, the limits of the wetting/drying apparatus, and the purpose of the test. The wetting/drying test, as discussed in the introduction, was intended to be a simulation of material saturation due to phenomena such as tidal fluctuation, wave splash, etc. Since high and low tides occur twice each day along the North Carolina coast, maximum daily wetting and drying would also occur twice each day. Considering the time available to the author for completion of this project, it was decided to simulate 18 months of field wetting and drying with 3 months of laboratory tests. This was accomplished by establishing a wetting cycle of 45 min. and a drying cycle expanded to 75 min. due to a drying temperature from the heat lamps of only 50^{o}C. With one complete cycle running two hours, twelve cycles could be completed in a 24 hr. period.

Once the test duration was determined, the number of specimens to be fabricated was calculated. With twelve samples per tank needed for each tensile test, thirty-six samples per tank would be needed if specimen examination was to be conducted at the end of each 30-day period. This number was compatible with the specimen's shape and the size of each tank.

Therefore, the test program consisted of a three month wetting and drying study of 72 specimens, (i.e., 36 specimens with the sea water tank and 36 specimens with the fresh water tank). The complete schedule of these specimens is given in Table 5. Twelve wetting/drying cycles were completed each day, and at the end of each month twelve specimens from both tanks were removed and loaded in tension to failure (see Figure 4). Six control specimens were fabricated and loaded in tension to failure without subjection to wetting and drying for later comparison (see Figure 5).

A visual examination of the specimens was made at periodic intervals. Several specimens were removed for x-ray diffraction and scanning electron microscopy analysis based upon these observations.

Thin cross-sections of the removed specimens located close to the plane of tensile failure were crushed to pass the #200 sieve for evaluation with the diffractometer. This powder was then carefully placed into aluminum sample holders in such a way as not to disturb the crystal orientation of the sample's surface. Each powder sample was subjected to x-rays emitted on the sample's

Table 5. Schedule of Asbestos Cement Specimens.

Months of Wetting/ Drying	Water Type	Sample Identification
1	Fresh Water	1-D, 2-D, 3-D, 4-D, 5-D, 6-D, 1-E, 2-E, 3-E, 4-E, 5-E, 6-E.
1	Sea Water	1-F, 2-F, 3-F, 4-F, 5-F, 6-F, 1-G, 2-G, 3-G, 4-G, 5-G, 6-G.
2	Fresh Water	1-H, 2-H, 3-H, 4-H, 5-H, 6-H, 1-I, 2-I, 3-I, 4-I, 5-I, 6-I.
2	Sea Water	1-J, 2-J, 3-J, 4-J, 5-J, 6-J, 1-K, 2-K, 3-K, 4-K, 5-K, 6-K.
3	Fresh Water	1-L, 2-L, 3-L, 4-L, 5-L, 6-L, 1-M, 2-M, 3-M, 4-M, 5-M, 6-M.
3	Sea Water	1-N, 2-N, 3-N, 4-N, 5-N, 6-N, 1-O, 2-O, 3-O, 4-O, 5-O, 6-O.

The samples were given the number of the sheet from which they were cut. The letters correspond to the water type and length of wetting/drying.

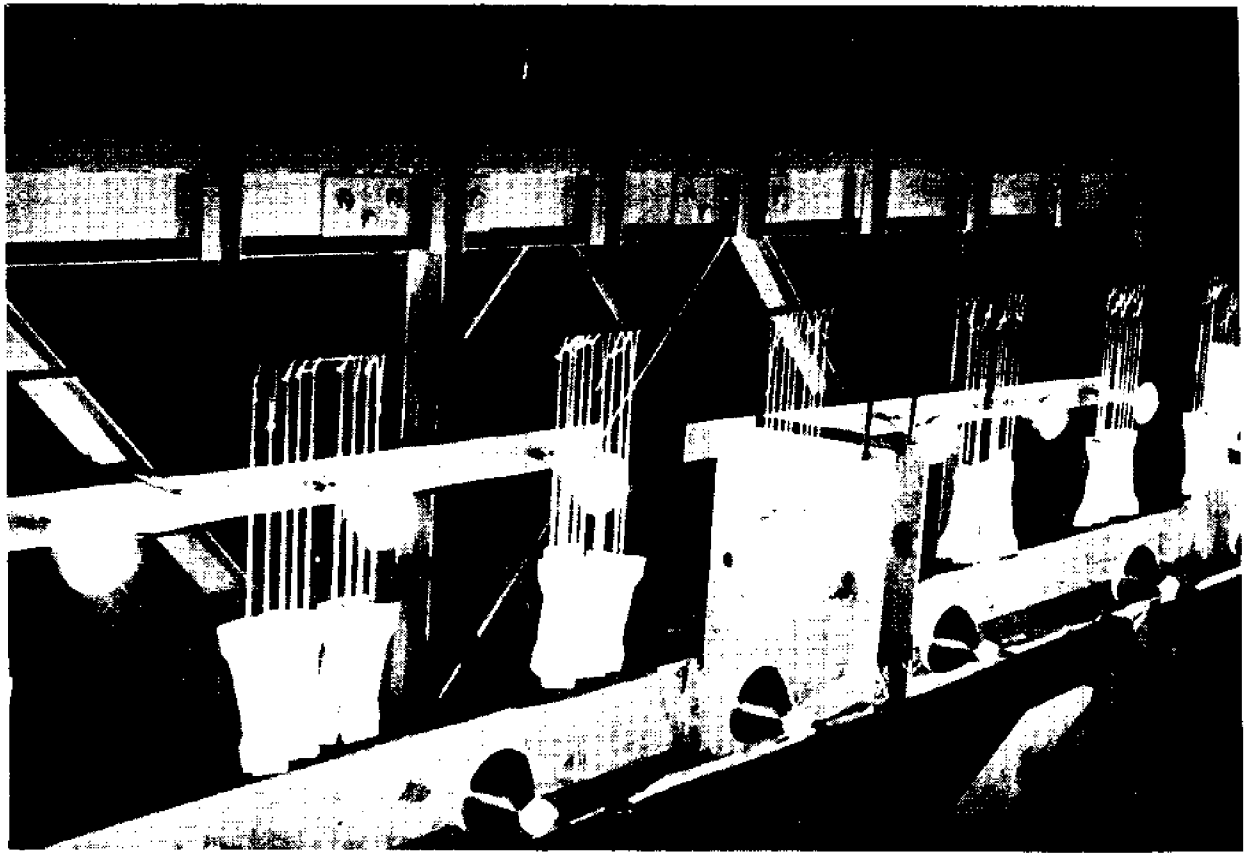

Figure 4. Wetting/Drying Apparatus at Beginning of Test Program. (Note: Drying Cycle).

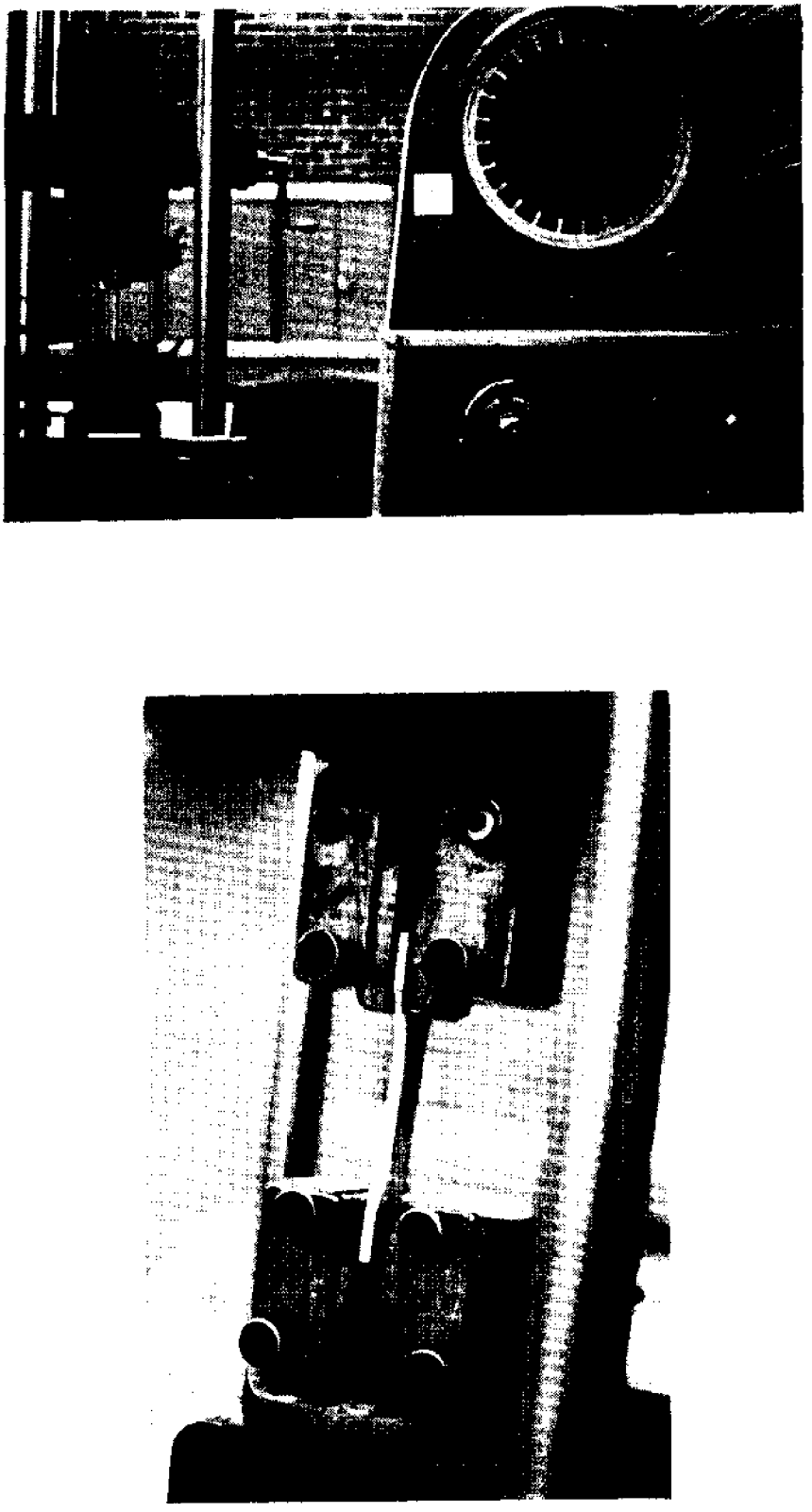

Figure 5. Southwark Loading Machine with Asbestos Cement Sample in Stocks.

surface over a 2θ range of 5^{o} to 55^{o}. Continuous peak intensities were monitored and recorded on graph paper for analysis. Compound identification was accomplished through the comparison of peak locations with known patterns for cement compounds and products of cement compounds exposed to sea water (Hadley, 1970).

A slow speed diamond saw was used for cutting smooth, polished cross-sections to be inspected at high magnification with the SEM. One specimen subjected to fresh water wetting/drying, three specimens subjected to one month, two months, and three months of sea water wetting/drying respectively, and one control specimen were observed at magnifications up to 50,000X. Special attention was given to any cracks or pores found in the specimens. In the cases of the samples exposed to one and three months of sea water wetting/drying and the original sample, an examination with the EDAX was performed for elemental comparison across the width of the samples. Each cross-section was divided into six equal segments, then each segement was focused in on and analyzed for its chemical composition.

All of the specimens were tested for absorption and specific gravity in general accordance with ASTM specification C 128-73 after the tensile strength test.

Asbestos Cement Bulkhead Sheet Obtained from the Field

Visual Examination of Field Samples. A segment of asbestos cement bulkhead was removed from a deteriorated canal retaining wall located near the Albemarle Sound (Outer Banks of North Carolina) (see Figures 6 through 10). This representative segment was one of several located along the bulkhead which had experienced

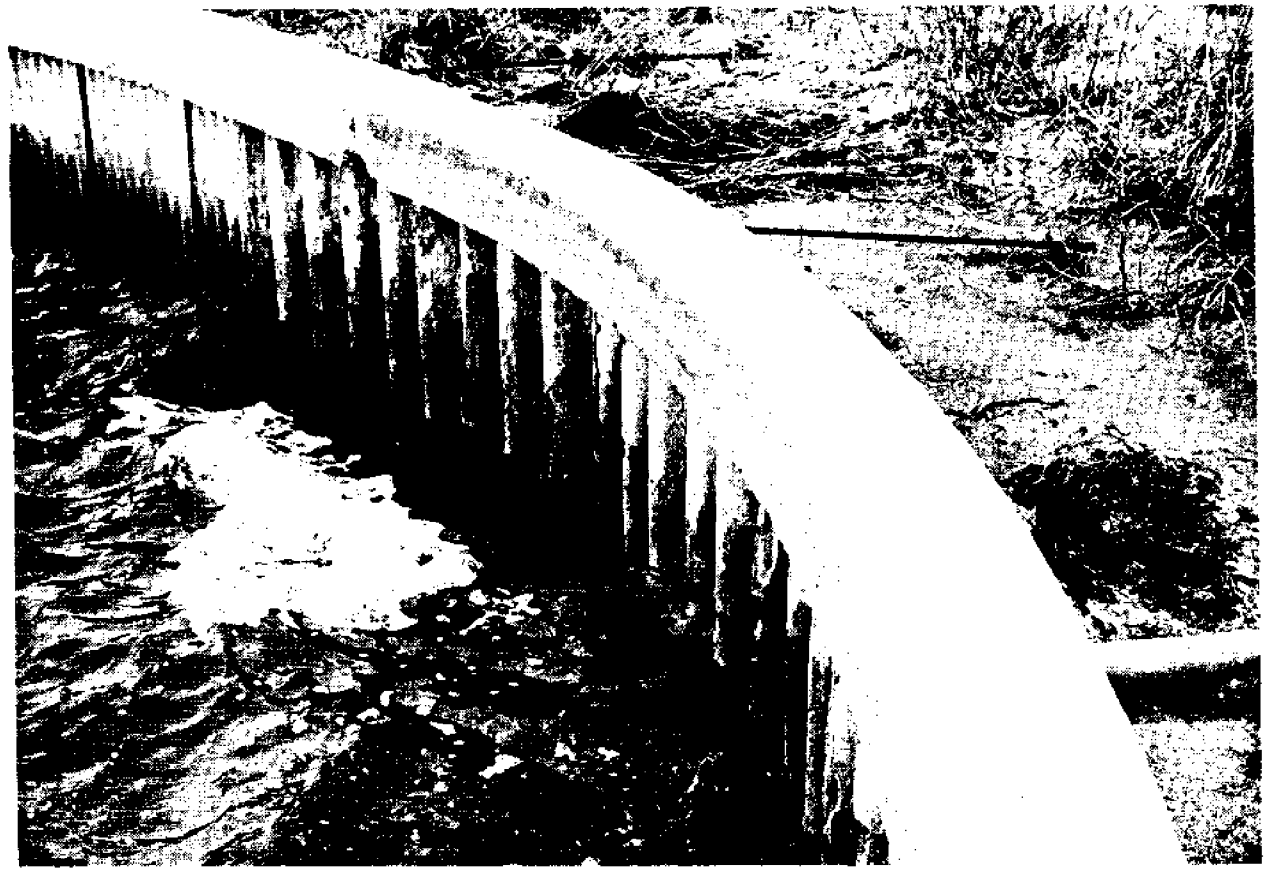

Figure 6. Asbestos Cement Bulkhead Located on the Outer Banks of North Carolina.

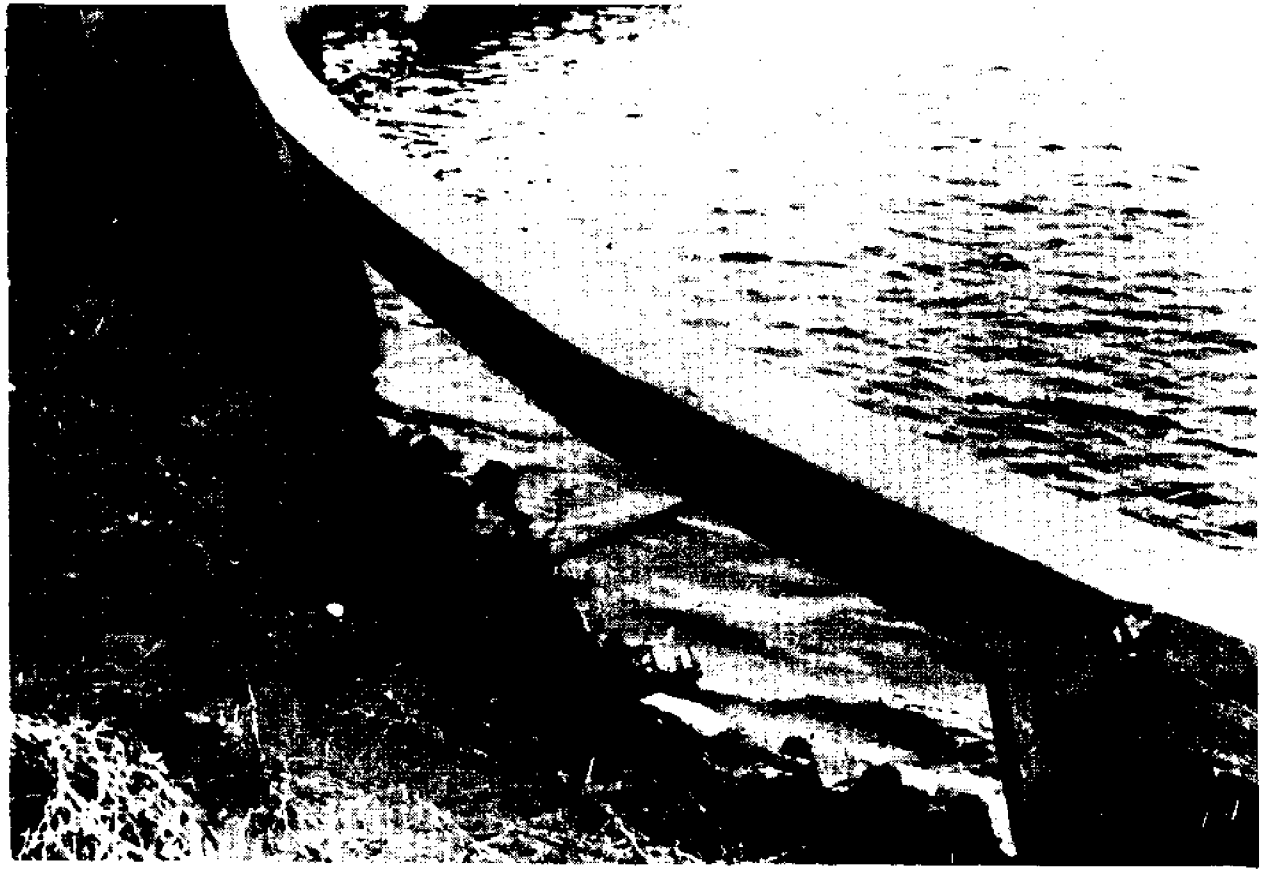

Figure 7. Corroded Section of Asbestos Cement Bulkhead.

Figure 8. Failure of Asbestos Cement Bulkhead and Concrete Cap.

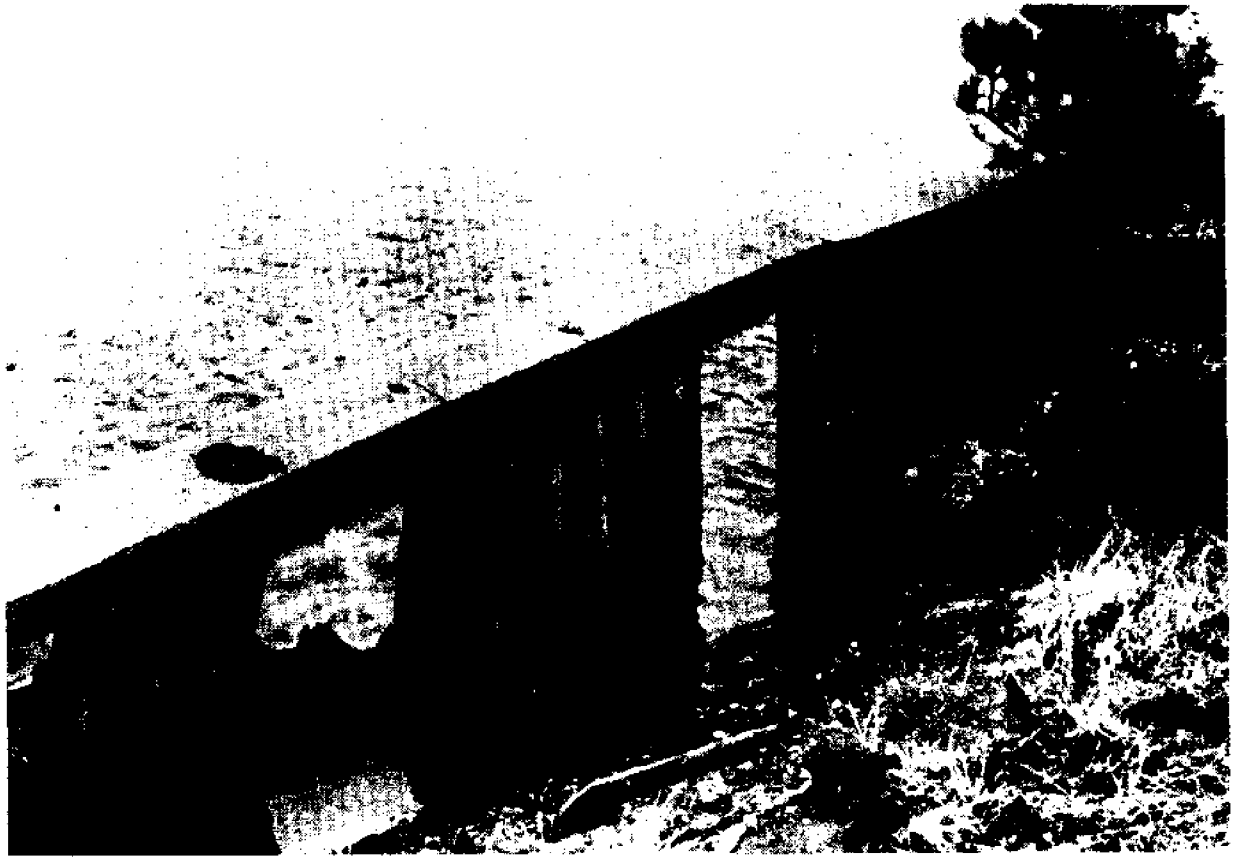

Figure 9. Asbestos Cement Bulkhead Deterioration.

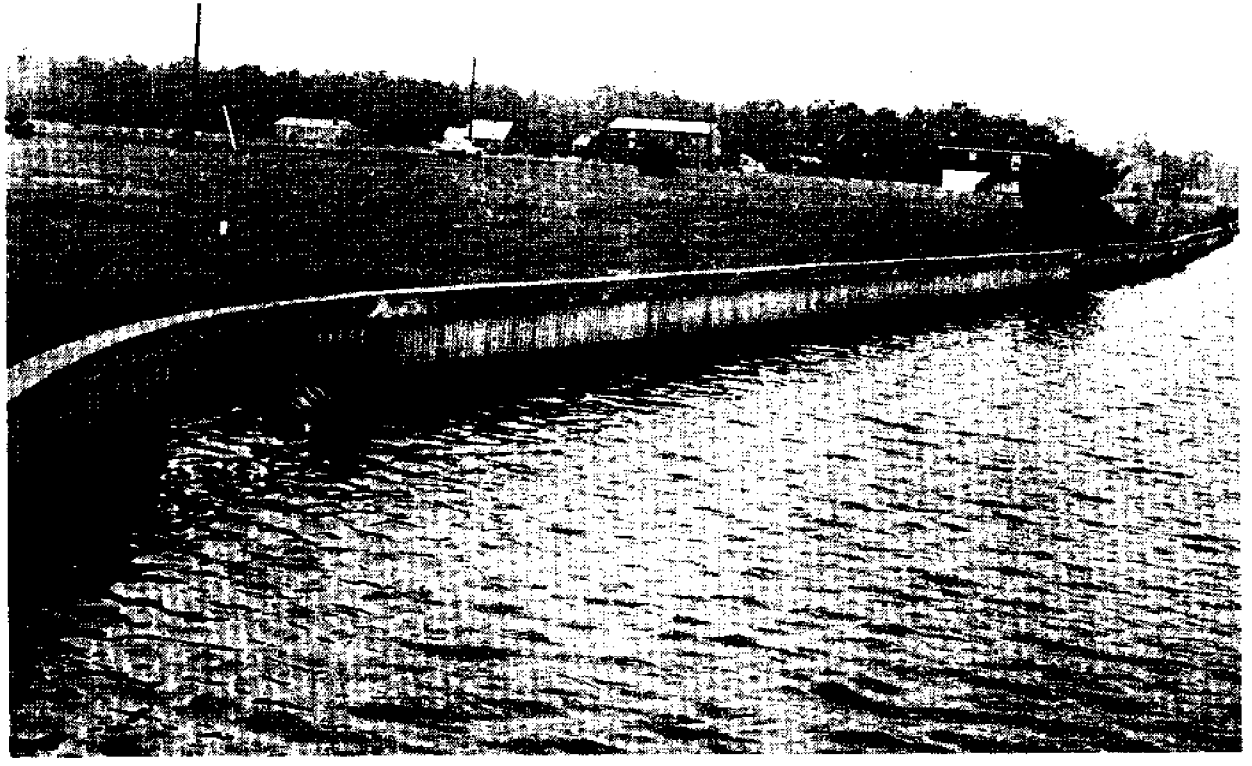

Figure 10. Section of Asbestos Cement Bulkhead from which Field Sample was Taken. (Note the relatively new bulkhead section which has replaced a badly deteriorated portion of the original structure.)

failure. This approximately 8-year-old bulkhead had been cured through the normal process. Its initial components consisted of chrysotile and Type II Portland cement with no additives. The bottom half of the sample had been in place below the low water level and had evidence of considerable biological growth on the forward face (see Figure 11). Just above this region was an area that had been subjected to a considerable splashing of the canal water and had a noticeable yellow stain on the surface facing the canal (see Figure 11). The top region of the sample was located approximately 90 cm (2.95 ft.) from the water surface and showed no signs of staining or biological growth (see Figure 11).

Field Specimen Strength Test. Four specimens were fabricated from the field sample into the same shapes as the laboratory specimens. One was taken from the top of the sample, one from the final specimen was taken from the extreme bottom of the sample. Barnacles and other biological growth were carefully removed from the surface of the specimens. Then each specimen was loaded in tension to failure.

Field Specimen X-Ray Diffraction Study. Powdered samples of the field specimens were prepared by grinding the material to pass the #200 sieve. Again, aluminum trays were used to hold the samples, which were run continuously through 2θ of 5° to 55°. Also, as before, relative peak intensities corresponding to 2θ angles were recorded on graph paper for later analysis.

a) Face of Samples Exposed to the Canal.

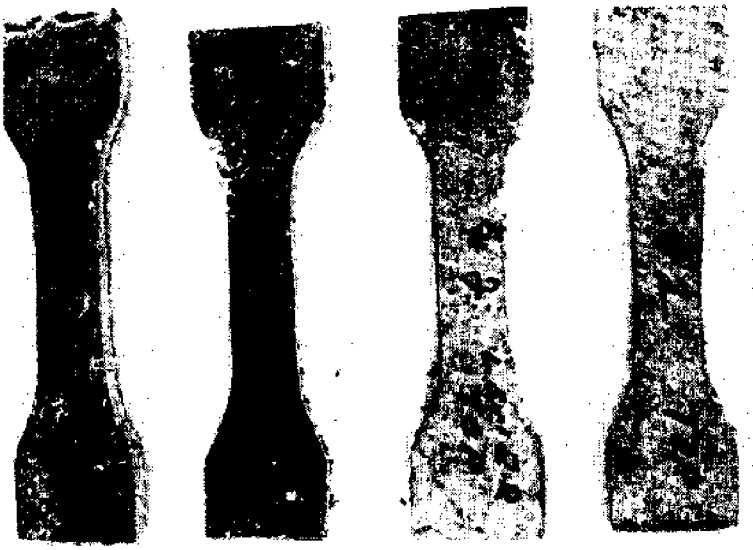

b) Backside of Samples Exposed to Backfill.

Figure 11. Specimens Cut from Field Asbestos Cement Sample.

Field Specimen Scanning Electron Microscope Study. The fractured surface of each field specimen was examined with the SEM for later comparison with the laboratory specimens. Also, thin cross-sections of the field specimens were cut and polished, then placed in the SEM for observations. Special attention was made in regards to the sample's denseness, its pore structure, and any fractures along the cross-section.

ANALYSIS OF DATA

Tensile Strength Results

The data obtained from the tensile strength tests is presented in Tables 8 through 14 in Appendix A, and a graph depicting the change in maximum stress with respect to time is shown in Figure 12. The majority of this data falls within the confidence interval of ± 190 N/cm^2 (0.045 lb./ft.^{2}) from the average stress of the control samples. However, different trends appeared at the end of each month of testing and varied between the samples tested in fresh water and those tested in seawater.

At the conclusion of the first month of wetting/drying, the samples tested in fresh water generally had a maximum tensile stress less than that of the control specimens, but still within the confidence interval. The samples tested in seawater , on the other hand, were found to have failed above the control stress and outside of the confidence interval in several cases.

Maximum stresses recorded after two months of testing displayed a wider range than at one month among the samples tested in seawater , while the samples tested in fresh water appeared to have gained considerably in tensile strength over samples at one month. The seawater samples were about evenly divided with stresses above and below the control stress. The majority of the fresh water samples failed at stresses greater than the control stress.

Data obtained after the third month of testing revealed a trend of weakening. Most of the samples failed at a stress less than the control stress, and many had stresses which fell outside

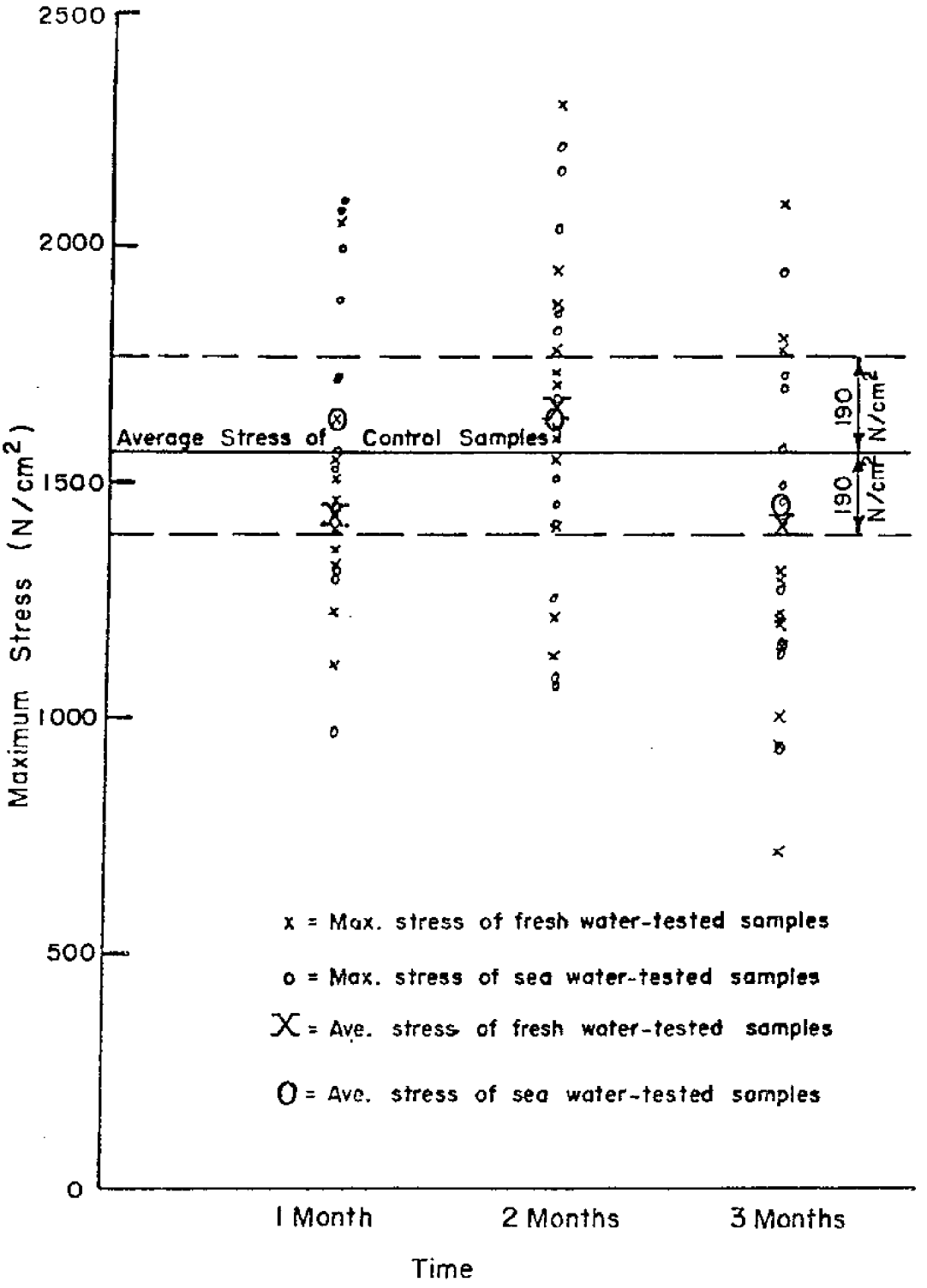

Figure 12. Strength of Laboratory Samples vs. Time.

of the confidence interval. The samples tested in both the fresh water and seawater tanks failed within the same general stress range.

The strength test on the field specimens revealed a marked difference between the specimens from the top portion of the bulkhead and those that had been continuously under water (see Table 6). The specimens from above the water line displayed even higher strength than the control samples of the laboratory asbestos cement material. Also, the data from the specimens below the water line indicated such a low stength that it is reasonable to consider that the cement remaining in the sample was not effective in a load bearing capacity. The stress that was carried must have been maintained by the asbestos fibers.

Table 6. Strength Results of Control and Field Samples.

	Samples					
	1	2	3	4	5	6
Strength (N/cm^2)	1778	1446	1457	1916	1673	1147
	1-top	2-top	3- Bottom		4- Bottom	
Strength (N/cm^2)	1922	1564	956		971	

X-Ray Diffraction Results

Several specimens were selected for further study with the diffractometer. One sample from each monthly group of seawater - tested specimens along with one sample which had been tested for three months in fresh water and one control sample were investigated. Also, each of the four field specimens was examined for composition.

Figure 13 illustrates the comparison of diffraction patterns obtained from samples 1, 3-G, 4-J, and 6-O (see Table 5). Silica is the dominant compound in all of these specimens having been added to the original mixture in a larger proportion than necessary to react with the liberated $Ca(OH)_2$. With the silica peaks dominating the diffraction pattern and strong background scatter, only those compounds which existed in relatively large quantities were identifiable. Also common in the diffraction patterns was the presence of $CaCO_3$ both as calcite and vaterite. A possible trace of CSH gel can be seen in the control specimen, although this is difficult to ascertain, considering the amount of background present. Gypsum can be found in an intensity close to that of $CaCO_3$ in all three of the seawater-tested specimens. However, the gypsum peaks did not appear in the control sample.

At one point in the third month of the wetting/drying test, the seawater level dropped just below the top surface of the specimens. As a result, the formation of salt crystals developed on the exposed surface of a few of the specimens. Along with the other diffraction patterns, a pattern was obtained for a portion of asbestos cement scraped from a region of crystal growth. When

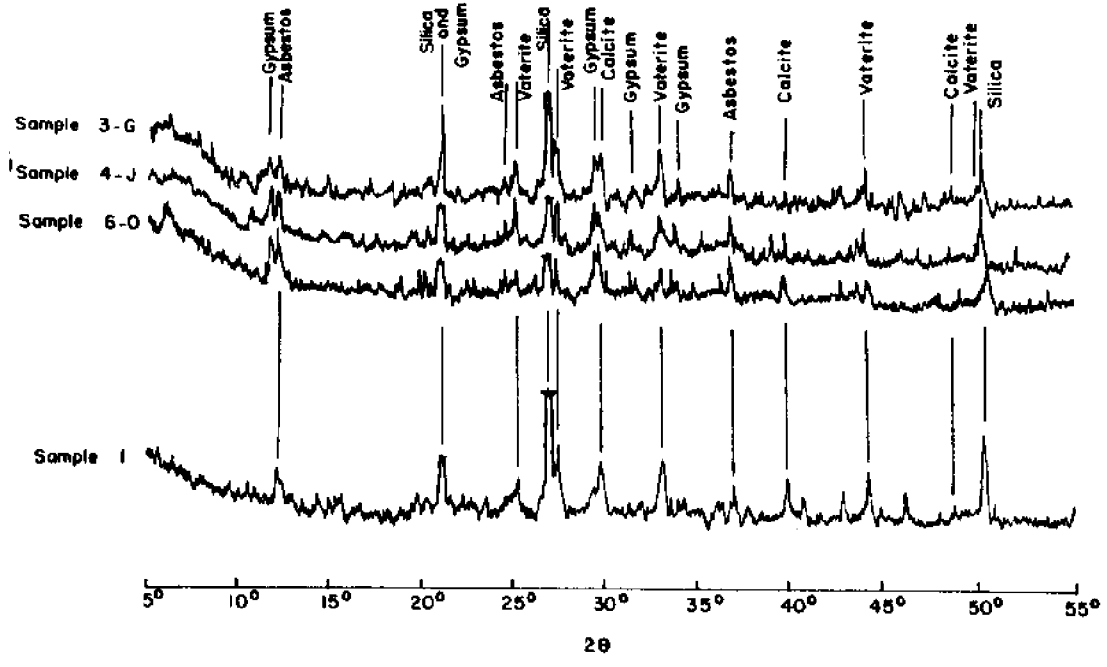

Figure 13. X-Ray Diffraction Patterns of 'Seawater -Tested Specimens vs. A Control Specimen.

compared with the results of a powdered sample taken from the fracture zone of the same specimen, this diffraction pattern exhibited three distinctly unique peaks as seen in Figure 14. A further investigation of these peaks with corresponding 2θ revealed that the salt was simply NaCl.

A comparison between the diffraction patterns of the four field specimens disclosed that they were all mainly composed of calcite and asbestos (see Figure 15). However, there was a distinct difference in the ratio of calcite intensity to asbestos intensity between the specimens from above the water line and those from below the water line. Calcite was present in an intensity sufficiently greater than asbestos in the top specimens, while this trend reversed itself in the specimens from the bottom half of the bulkhead.

Observations with the Scanning Electron Microscope

Each of the samples analyzed by the diffractometer for identification was also examined with the SEM for evidence of fracture formation as well as crystal structure. Cracks were found to have penetrated from the sample's edge to a depth of about 0.30 cm (0.12 in.) in specimen 6-0. Also, cracks were beginning to form along the edge of sample 4-J. However, in neither case was there evidence of expansive salt crystal growth in the cracks. In both specimens, the cracks were widest at the edge and tapered off into a series of smaller fractures. With the EDAX it was determined that the control sample, 1, as well as samples 5-0 and 6-0 contained the elements common to asbestos cement in what appeared to be the proper proportions (see Table 7). However, sulfur appeared in a significant amount on the edges of sample 5-G and throughout the

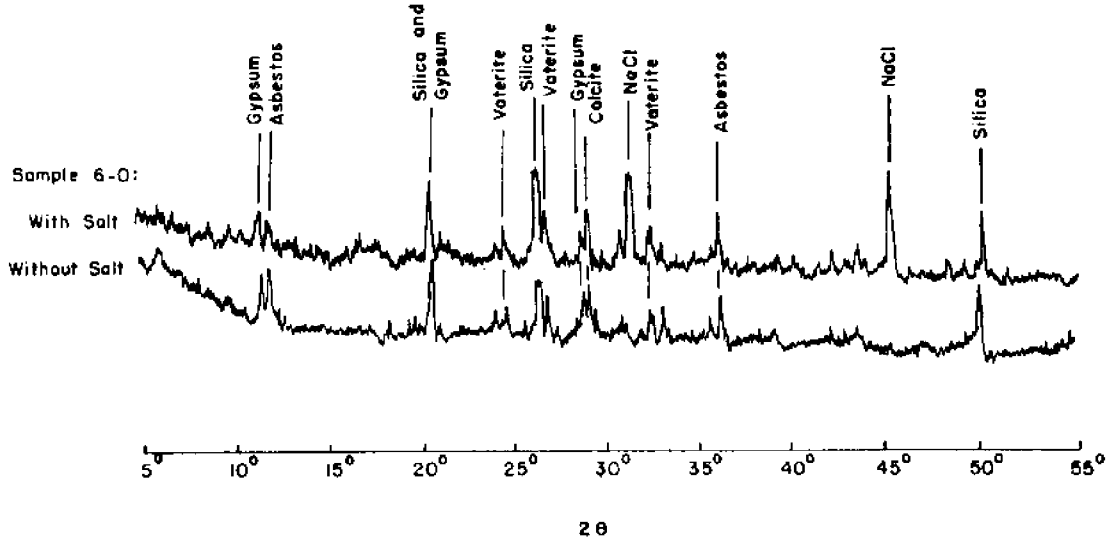

Figure 14. X-Ray Diffraction Patterns of Sample 6-0 With and Without External Salt Crystals.

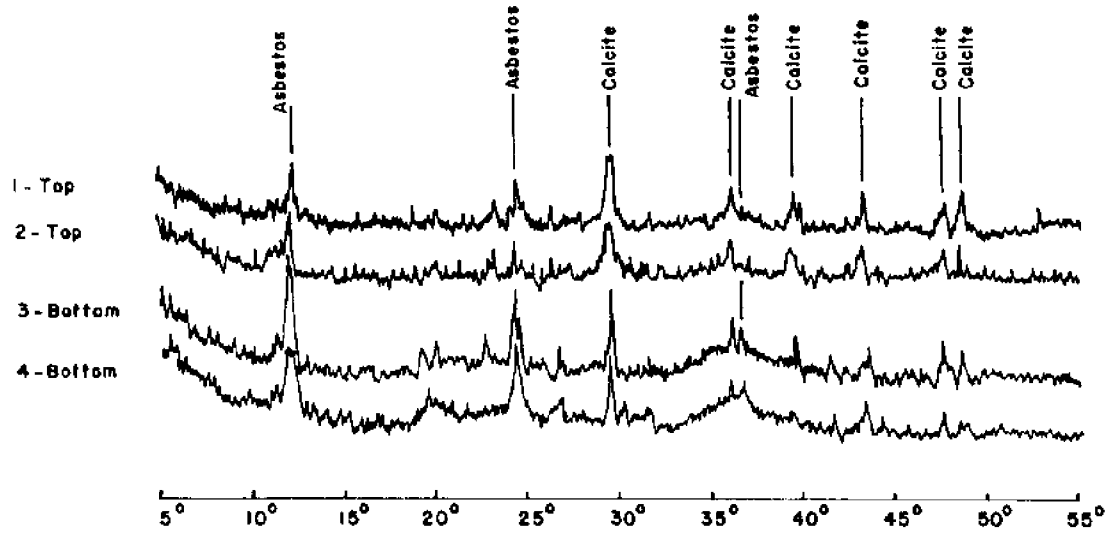

Figure 15. X-Ray Diffraction Patterns of Field Specimens.

Table 7. EDAX Examination of Asbestos Cement Specimens.

Sample	Section	Percent of Total Integral Count*					
		Mg	Si	S	Cl	Ca	Fe
1	1	2.1	37.8	-	-	58.2	1.8
	2	1.5	37.4	-	-	59.4	1.7
	3	1.9	36.6	-	-	59.6	1.9
	4	1.2	37.5	-	-	59.6	1.7
	5	1.5	36.0	-	-	60.8	1.7
	6	1.1	34.8	-	-	62.2	1.9
5-G	1	3.2	37.2	2.2	0.9	55.0	1.4
	2	2.1	38.1	0.9	1.6	55.7	1.6
	3	2.4	37.7	-	1.6	56.5	1.8
	4	1.9	38.8	-	1.8	55.8	1.7
	5	2.0	38.7	0.8	1.8	55.3	1.3
	6	2.1	34.3	1.7	0.8	58.6	2.4
6-0	1	0.8	30.9	2.5	1.0	63.3	1.5
	2	1.3	35.5	1.6	1.6	58.1	1.9
	3	1.7	36.2	1.0	1.0	57.9	2.1
	4	2.0	37.3	0.9	1.2	56.5	2.1
	5	2.4	33.2	5.6	0.8	55.6	2.4
	6	1.1	29.8	6.3	1.3	59.2	2.3
Crack A-1 of Sample 6-0		0.7	15.6	12.5	-	70.7	0.5
Crack A-2 of Sample 6-0		1.1	28.3	12.0	-	57.4	1.2

* For example, sample , section 3 had a total integral count of 42,503 with a count of 752 for Magnesium, or 2.1%, a count of 15,567 for silicon, or 36.6%, etc.

cross-section of sample 6-0, but did not occur at all in the control specimen. This finding concurred with the x-ray diffraction results which revealed the presence of gypsum in the specimen. A closer examination of some of the cracks found in sample 6-0 turned up a high concentration of sulfur from within the cracks. This data is also displayed in Table 14 with pictures of the corresponding cracks shown in Figure 16. Along with sulfur, chlorine was found in fairly even amounts throughout the cross-sections of samples 5-G and 6-0 as expected. Little or no chlorine was detected in the region of the cracks.

Water Analysis

Water samples were obtained from four different locations for analysis relating to laboratory test results. Fresh water used in the wetting/drying test was water drawn directly from the tap and was not considered to contain any substances which of themselves corrode cement products. The seawater which was used in the wetting/drying test was collected from a sound along the southern coast of North Carolina within one mile of an inlet. The water from which the field samples were removed was located in a canal which is off a sound along the northern North Carolina coast. This canal was several miles from the nearest inlet. The final water sample considered was the seawater used in the wetting/drying apparatus after three months of testing.

As an estimate of how well the laboratory test represented the conditions in the field, comparisons were made between the canal water and the seawater originally used in the laboratory. Since only a relative distinction between the samples was needed,

a) Crack A-1, 100X.

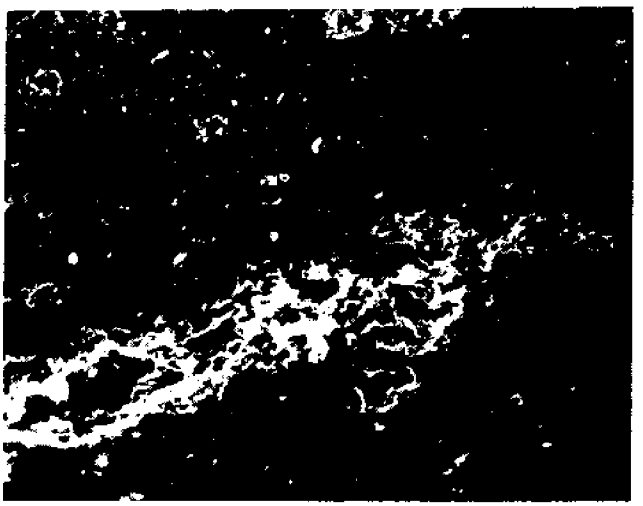

b) Crack A-2, 100X.

Figure 16. Internal Cracks of Specimen 6-0 Containing High Amounts of Sulfur.

salinities were gauged by a conductivity bridge, with the results indicating that the laboratory seawater was about five times as saline as the canal water. This is not unexpected when considering the locale of the samples in relation to their nearest inlets, which are the salt source for the sounds. Also, a test for sulphates was conducted on these water samples. The canal water was found to contain 180 ppm SO_4, while the laboratory seawater contained 2760 ppm SO_4. From the degree of sulphate aggressivity shown in Table 2, the laboratory seawater is in the range of severe attack, but the canal water is considered to be only slightly capable of sulphate attack.

In an effort to determine the presence of calcium which could have been leached out of the cement and into the water, relative quantities of calcium contained in the water samples were measured by the ratio Ca/Na (see Table 8). The laboratory seawater after three months of wetting/drying contained almost twice as much calcium as it did originally. This is evidence that some type of exchange took place during the wetting and drying cycles to form a calcium compound which is readily soluble in seawater. Although the Ca/Na ratio in the field samples is greater than that found in the original laboratory seawater, it is difficult to determine by this test that calcium compounds are being dissolved into the water, because dilution in the canal would be so great that any change in calcium concentration would be indetectable.

The final tests of water quality were those of pH and free CO_2 content. A pH value was determined for the fresh water and the laboratory seawater before and after wetting/drying. These

Table 8. Ca/Na Ratio of Water Samples.

Identification of Water Samples	Test #	Ca (mg/l)	Na (mg/l)	Ca/Na
Canal Water	1	30.6	6800	0.0045
	2	30.2	6900	0.0044
	3	30.3	7000	0.0043
Original Laboratory Seawater	1	38.1	10,700	0.0036
	2	37.4	10,800	0.0035
	3	37.7	11,000	0.0034
Laboratory Seawater After Testing	1	66.9	10,900	0.0061
	2	65.6	10,800	0.0061
	3	65.1	10,900	0.0060

values approached 8.0 in all three water samples, and therefore, each was determined non-aggressive in terms of carbonic acid attack. However, to calculate the pH and CO_2 values of the canal water, tests had to be performed at the field site to avoid any change in results due to shaking the sample of atmospheric exposure. These tests indicated the presence of about 140 mg/L of free CO_2 and a pH of 6.8. Although measurements were not accurate enough to determine the aggressive portion of the free CO_2 in the canal, water containing free CO_2 at a pH below 7 is capable of aggressive action on cement.

Temperature Variations in the Field

Freezing and thawing action is considered to be very detrimental to concrete. However, within the scope of this project, only application along the North Carolina coastline of asbestos cement bulkheads is being examined. A history of temperature variations in this region revealed that in the past eight years, the period in which asbestos cement has been increasingly used, the temperature dipped below $10^{\circ}F$ only twice. At no time was the temperature below $32^{\circ}F$ for an entire 24 hr. period (USWS, 1978). Therefore, it was decided that freezing and thawing were not instrumental in the corrosion of asbestos cement bulkheads along the coast of North Carolina.

Physical Examination of Field and Laboratory Asbestos Cement Specimens

Upon examination of both field and laboratory specimens, several observations were made which offered evidence of material deterioration. One of the first noticeable changes that occurred

was hairline fractures along the edges of the laboratory specimens tested in seawater (see Figures 17 and 18). These cracks developed between the first and second months of wetting/drying, and became extensive by the end of the third month of testing. Also, the surface of these samples became increasingly powdery with a bleached appearance. Neither the cracks, the powdery surface, nor the bleaching were apparent in the samples tested with fresh water, even after three months of wetting/drying.

The soft powdery surface was also evident in the field specimens. Again, however, distinction arose between specimens taken from above the water line and those from below the water line. Although there was some surface softening of asbestos cement above the water line, the material appeared very solid. Asbestos cement from below the water line, on the other hand, gave an appearance of extensive deterioration, having degenerated to a loosely packed, fibrous consistency. The face of the material exposed to the canal was covered with barnacles.

Absorption and specific gravity tests were conducted for an estimation of porosity among the samples (see Table 17 in Appendix A). The results revealed that all of the specimens had a fairly high rate of absorption in comparison with what is considered sound concrete in a marine environment (around 20% compared to 6 or 7%). However ,in the two field specimens from below the water line, absorption increased to more than 50%, while the specific gravity dropped appreciably. This confirmed the highly leached state of the material which was suspected by observations.

Figure 17. Edge of Asbestos Cement Sample After Two Months of Wetting/Drying in Seawater.

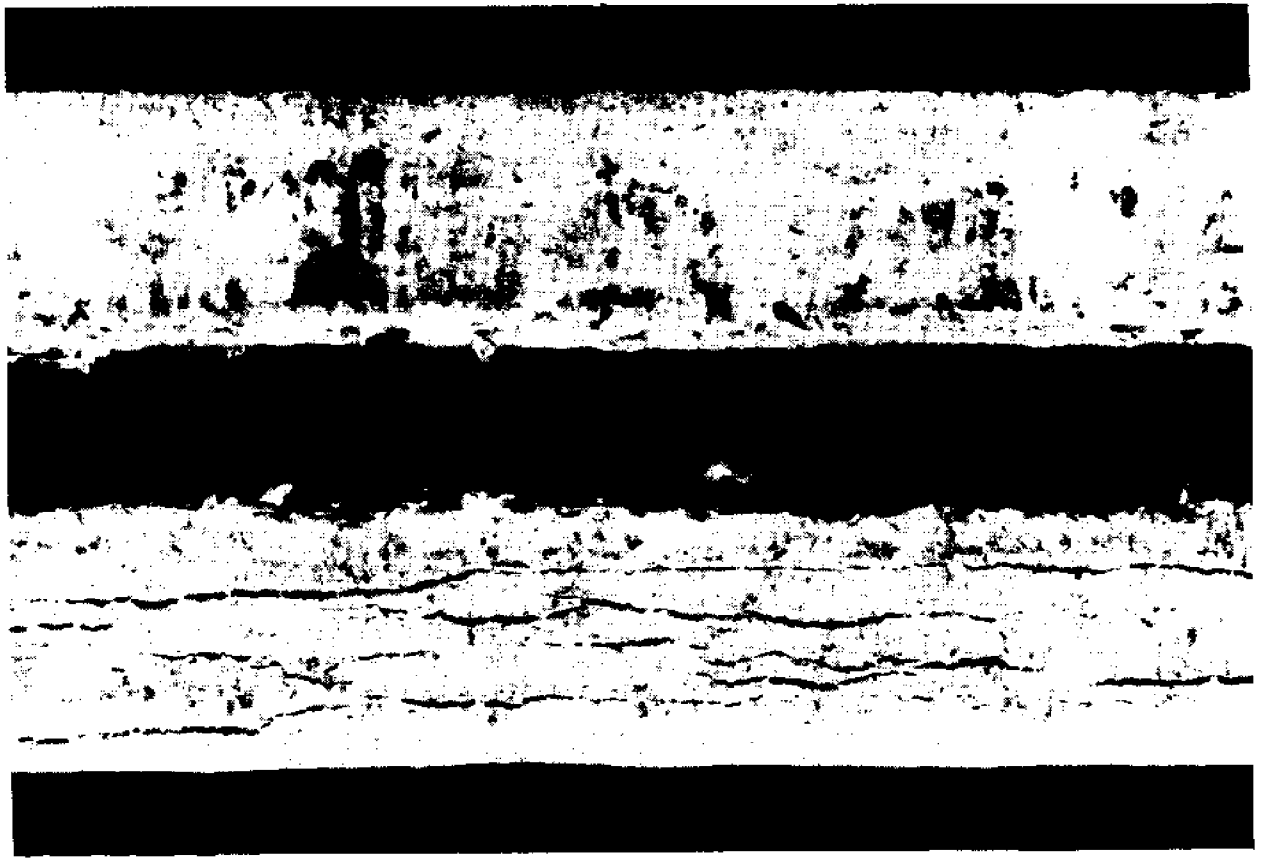

Figure 18. Comparison of Asbestos Cement Sample After Three Months of Wetting/Drying in Fresh Water (top) with Sample After Three Months of Wetting/Drying in Seawater.

DISCUSSION OF RESULTS

Cement is susceptible to deterioration by many corrosive agents, including carbonic acid, sulphates, and leaching which have been investigated. Evidences of these types of corrosion have occurred in both the field and laboratory specimens. The means of deterioration progression, however, appear to be different between the field and the laboratory.

The Processes of Asbestos Cement Deterioration in the Field

The results of the various tests on the field specimens indicated that the material originating from below the water line had little structural integrity remaining. The relatively high porosity of the material allowed for extreme percolation. Also, with the thickness of the asbestos cement sheet being only 0.95 cm (0.375 in.) this percolation was allowed to flow through the entire cross-section in probably a very short time. Since the material was not autoclaved, there was a possibility of some free $Ca(OH)_2$ existing in the asbestos cement. Barring complete carbonation through atmospheric CO_2 before placement in the canal, this $Ca(OH)_2$ could easily have been leached out of the bulkhead, taking away a portion of the structure's mass.

Based upon the ACI limits to avoid sulphate aggressivity, corrosion of the asbestos cement by sulphate salts can be disregarded due to the low sulphate concentration of the canal water. X-ray diffraction patterns failed to indicate any peaks which can be attributed to the common sulphate salts (i.e., ettringite and gypsum) to substantiate these results. Also, the lack of cracks

either along the surface of the material or visible through the SEM gives further proof to the absence of expansion, which is common to sulphate attack.

Carbonic acid attack is considered the principal cause of deterioration of the asbestos cement bulkhead from the field. Analysis of the canal water revealed a high enough free CO_2 level existing in the presence of acidic water to attack the cement by the process mentioned by Biczok (1967). A look at the x-ray diffraction patterns indicated that $Ca(OH)_2$ was absent, at least in significant quantity. By the presence of extensive amounts of calcite, it can be concluded that the free $Ca(OH)_2$, present as a hydration product, reacted with atmospheric CO_2 to form $CaCO_3$. Since $CaCO_3$ is most stable in the form of calcite, the absence of the polymorphs vaterite and aragonite suggests that the $CaCO_3$ had been formed for quite some time. The change in the intensity ratio of calcite with respect to asbestos above and below the water line indicates that the $CaCO_3$ is being dissolved through some process. Calcite itself is highly insoluble even in seawater , but in the presence of aggressive CO_2 it is capable of dissolving in the form of the bicarbonate, $Ca(HCO_3)_2$, which is so soluble in saline water that it will likely dissolve directly upon formation in seawater . The SEM confirmed the fibrous appearance of the specimens from below the water surface due to loss of calcite, which, according to the diffraction patterns, had become the only cementing constituent of the material.

The Processes of Asbestos Cement Deterioration in the Laboratory

The results of the tests conducted on the laboratory specimens did not present as clear cut a solution as those for the field specimens. Although the seawater-tested specimens exhibited tensile strengths on the same order as those tested in fresh water, the presence of hairline fractures along the edge of the samples exposed to seawater for greater than one month was plainly an indication of some form of aggressive attack on the cement. Also, the increase in the amount of calcium in the seawater due to wetting/drying of the cement pointed to a reaction of the insoluble calcium compounds to form a more soluble compound.

Carbonation is ruled out in this case, as the water is an alkaline solution. Also, the x-ray diffraction patterns showed no significant change in the intensity of $CaCO_3$ with time other than the transition from vaterite to calcite.

Sulphate attack of the ettringite form is not evident by either the diffraction patterns or observations with the SEM. Ettringite's largest diffraction peak occurs at 9^{o}, 2θ, and it is clear from Figure 13 that no identifiable peak is present at this angle in any of the seawater-tested specimens. With the SEM an examination at high magnification of the hairline fractures found in samples 6-0 and 5-J was possible. However, neither the needle-like structure of ettringite nor expansive crystal formation inside the cracks were observed.

The lack of expansive crystals also ruled out the classical form of gypsum attack on the cement. Yet, gypsum was clearly evident in the seawater samples, while none was exhibited in the

control material. Historically, it has been assumed that the presence of $Ca(HO)_2$ is essential to the formation of gypsum in cement. With the asbestos cement tested in the laboratory having been cured in an autoclave, there should have been no $Ca(OH)_2$ available to react with the sulphates through this process. X-ray diffraction patterns further substantiated this by a lack of $Ca(OH)_2$ in the control samples. Therefore, gypsum must have been formed through a reaction which is unknown to the author.

Comparison Between Field and Laboratory Results

The data from the field and laboratory tests leads to different conclusions. This can be attributed in part to the difference in the SO_4 and CO_2 content and pH of the seawater used in the laboratory test as compared to those characteristics of the canal water. Other variations in the results can be attributed to idealized conditions in the laboratory, where free CO_2 could not be formed as in the field, and the use of an autoclaved product in the laboratory, when the field material had been normally cured. One factor involving the lack of a definite corrosion pattern through the results of the laboratory test was the short length of time of the testing. A longer test might have led to a better understanding of the destructive processes which caused the formation of hair-line cracks in the asbestos cement specimens.

SUMMARY AND CONCLUSIONS

Summary

Tests were conducted to determine the performance of asbestos cement used in bulkhead/retaining structures along the coastline of North Carolina. The study included a three-month laboratory wetting/drying test, an examination of a deteriorated asbestos cement bulkhead from the field, and analysis of material tensile strength, water quality, and absorptive properties of the material, and tests for material composition through x-ray diffraction and scanning electron microscopy.

Conclusions

1. The asbestos cement bulkhead under investigation from the field was severely deteriorated through the reaction of aggressive CO_2 with $CaCO_3$ in the material. The $Ca(HCO_3)_2$ which was formed was leached out of the structure in solution, thus causing a drop in material density and increase in porosity.
2. As reported in the literature and substantiated by the study, asbestos cement bulkheads are vulnerable to carbonic acid attack in canals and estuaries where biological decay produces an excess of dissolved CO_2 and the water's pH is less than 7.
3. Autoclaved asbestos cement as opposed to normally and asbestos cement may be helpful in delaying extensive deterioration due to carbonic acid. It contains a high amount of silica which is non-reactive at normal temperatures.
4. Autoclaved asbestos cement is subject to corrosion in sea-water. The cause of this corrosion is debatable, but it is likely

that the presence of a sulphate concentration along with the wetting/drying process invoked by tidal action plays a major role in the mechanism of deterioration.

RECOMMENDATIONS FOR FUTURE CONSIDERATION

1. A prolonged wetting/drying study in the laboratory to simulate up tc 5 years in the field should be conducted for a better understanding of the mechanisms of corrosion of autoclaved asbestos cement.

2. An investigation into possible coatings for asbestos cement products needs to be carried out.

3. A laboratory study to confirm the limits of CO_2 attack should be accomplished. In addition, a more thorough analysis of the aggressive pH and CO_2 levels in the field should be accomplished.

4. A freeze/thaw study should be made to determine the durability of asbestos cement in cold climates.

LITERATURE CITED

ARNI, H. T., 1972. "Resistance of Concrete to Weathering", Significance of tests and properties of concrete and conrete-making materials, STP 169-A, ASTM, pp 261-274.

ATWOOD, A. and W. JOHNSON, 1924. "The Disintegration of Cement in Sea Water," Transactions, ASCE, Vol. 87, pp 204-230.

BICZOK, I., 1967. Concrete Corrosion - Concrete Protection Chemical Publishing Company, New York, N.Y.

BOWLES, O., 1937. "Asbestos", Bulletin No. 403, Bureau of Mines, U.S. Department of the Interior.

COLE, W.F. and B. KROONE, 1960. "Carbon Dioxide in Hydrated Portland Cement", Proceedings, ACI Journal, Vol. 56, pp. 1275-1295.

Committe 201 Report, 1977. "Guide to Durable Concrete", Proceedings, ACI Journal, Vol. 74, No. 12, pp. 573-609.

CZERNIN, W., 1962. Cement Chemistry and Physics for Civil Engineers, Chemical Publishing Company, New York, N.Y.

HADLEY, D.W., 1970. Selected X-Ray Diffraction Patterns of Cement Compounds and Salts, Purdue University.

IDORN, G.M., 1964. "A Concrete Jetty With Frost Damage", Magazine of Concrete Research, Vol. 16, No. 47, pp. 89-92.

KALOUSEK, G.L., F.V. CAMARDA, J.E. KOPANDA and Z.T. JUGOVIC, 1966. "Analysis of Asbestos Cement Binders", Materials Research and Standards, Vol. 6, No. 4, pp. 169-179.

KENNEDY, T.B. and K. MATHER, "Correlation Between Laboratory Accelerated Freezing and Thawing at Treat Island, Maine", Proceedings, ACI Journal, Vol. 50, pp. 141-172.

LEA, F.M., 1970. The Chemistry of Cement and Concrete, 3rd Edition, Edward Arnold Limited, London, England.

META, P.K. and H.H. HAYNES, 1975. "Durability of Concrete in Sea Water", Journal of the Structural Division, ASCE, Vol. 101, pp. 1679-1686.

POWERS, T.C., 1962. "A Hypothesis on Carbonation Shrinkage", Journal of the Research and Development Laboratory, PCA, Vol. 4, No. 2, pp. 40-50.

SAUMAN, F., 1971. "Carbonization of Porous Concrete and its Main Binding Components", Cement and Concrete Research, pp. 645-666.

SHIDELER, J.J., 1963. "Carbonation Skrinkage of Concrete Masonry Units", Journal of the Research and Development Laboratories, PCA, Vol. 5, No. 3, pp. 36-51.

SVERDRUP, H. U., M. M. JOHNSON and R.H. FLEMING, 1948. The Oceans, Prentice -Hall Englewood Cliffs, N.J.

TERZAGHI, R. D., 1948. "Concrete Deterioration in a Shipway", Proceedings, ACI Journal, Vol. 44, pp. 977-1005.

TERZAGHI, R.D., 1949 "Concrete Deterioration Due to Carbonic Acid", Journal of the Boston Society of Civil Engineers, ASCE, Vol. 36, pp. 136- .

TREMPER, B., 1936. "The Effect of Acid Waters on Concrete", Proceedings, ACI Journal, Vol. 28, pp. 1-32.

U.S. Weather Service, 1978. "Climatological Data: North Carolina", NOAA, Vol. 83.

VERBECK, G., 1958. "Carbonation of Hydrated Portland Cement", STP - 205, ASTM.

WAKEMAN, C.M., 1958. "Use of Concrete in Marine Environments", Proceedings, ACI Journal, Vol. 54, pp. 841-856.

WALDOLE, R.E. and R.H. MYERS, 1972. Probability and Statistics for Engineers and Scientists, MacMillan Publishing Company, New York, N.Y.

Appendix A.

Test Data and Selected Results

Table 9. Strength Test: Preliminary Wet/Dried Samples.

	Samples					
	1-A	1-B	2-A	2-B	3-A	3-B
Width (cm)	2.58	2.60	2.61	2.62	2.59	2.57
Thick. (cm)	0.848	0.813	0.833	0.841	0.848	0.838
Area (cm^2)	2.19	2.12	2.17	2.20	2.19	2.15
Force (N)	3514	2309	2593	3781	3941	3461
Strength (N/cm^2)	1607	1091	1193	1719	1797	1606
	4-A	4-B	5-A	5-B	6-A	6-B
Width (cm)	2.60	2.58	2.56	2.63	2.70	2.55
Thick. (cm)	0.798	0.813	0.818	0.836	0.823	0.861
Area (cm^2)	2.07	2.10	2.09	2.20	2.22	2.19
Force (N)	1975	2985	3114	2126	3714	2135
Strength (N/cm^2)	954	1424	1489	967	1673	974

Mean Stress = 1375 N/cm^2

Standard Deviation = 292.64 N/cm^2

Table 10. Strength Test: Preliminary Control Samples.

	Samples					
	1-C	1-D1	2-C	2-D1	3-C	3-D1
Width (cm)	2.55	2.64	2.53	2.46	2.62	2.56
Thick. (cm)	0.856	0.808	0.831	0.813	0.836	0.810
Area (cm^2)	2.18	2.14	2.10	2.00	2.19	2.08
Force (N)	2669	3336	3398	3492	*	3029
Strength (N/cm^2)	1220	1562	1616	1746	*	1453
	4-C	4-D1	5-C	5-D1	6-C	6-D1
Width (cm)	2.65	2.53	2.51	2.58	2.57	2.52
Thick. (cm)	0.836	0.818	0.826	0.828	0.826	0.833
Area (cm^2)	2.21	2.07	2.07	2.14	2.12	2.10
Force (N)	3171	3016	3527	3732	3674	3581
Strength (N/cm^2)	1433	1456	1703	1742	1735	1708

Mean Stress = 1600 N/cm^2
Standard Deviation = 128.74 N/cm^2

* The machine was reloaded before the force value of sample 3-C could be read.

Table 11. Tensile Strength Results of Test Samples, First Group, Fresh Water.

	Sample					
	1-D	1-E	2-D	2-E	3-D	3-E
Width (cm)	2.51	2.57	3.02	2.79	2.59	2.72
Thick. (cm)	0.859	0.853	0.848	0.820	0.881	0.856
Area (cm^2)	2.16	2.19	2.56	2.29	2.28	2.33
Force (N)	2936	4492	4181	3314	3536	3514
Strength (N/cm^2)	1360	2052	1631	1446	1549	1510
	4-D	4-E	5-D	5-E	6-D	6-E
Width (cm)	2.62	3.12	2.67	2.69	2.84	2.59
Thick. (cm)	0.874	0.808	0.843	0.843	0.815	0.826
Area (cm^2)	2.28	2.52	2.25	2.27	2.32	2.14
Force (N)	2558	3603	3158	3247	3114	2647
Strength (N/cm^2)	1119	1428	1405	1430	1342	1238

Table 12. Tensile Strength Results of Test Samples, First Group, Seawater.

	Sample					
	1-F	1-G	2-F	3-F	3-F	3-G
Width (cm)	2.57	2.54	2.64	2.77	2.72	2.72
Thick. (cm)	0.876	0.853	0.813	0.826	0.831	0.874
Area (cm^2)	2.25	2.17	2.15	2.28	2.26	2.37
Force (N)	4226	3670	3336	4759	3425	3247
Strength (N/cm^2)	1880	1693	1554	2082	1517	1367
	4-F	4-G	5-F	5-G	6-F	6-G
Width (cm)	2.57	2.39	2.79	2.49	2.57	2.64
Thick. (cm)	0.787	0.851	0.777	0.846	0.841	0.815
Area (cm^2)	2.02	2.03	2.17	2.10	2.15	2.15
Force (N)	4025	2936	3692	2691	2313	4448
Strength (N/cm^2)	1993	1445	1700	1278	985	2065

Table 13. Tensile Strength Results of Test Samples, Second Group, Fresh Water.

	Sample					
	1-H	1-I	2-H	2-H	3-H	3-I
Width (cm)	2.44	3.81	2.74	2.69	2.77	2.51
Thick. (cm)	0.843	0.907	0.823	0.841	0.859	0.826
Area (cm^2)	2.06	3.46	2.26	2.26	2.37	2.08
Force (N)	4737	4826	4226	3647	3714	3692
Strength (N/cm^2)	2304	1397	1872	1611	1562	1779
	4-H	4-I	5-H	5-I	6-H	6-I
Width (cm)	3.40	2.84	2.59	2.62	2.62	2.69
Thick. (cm)	0.818	0.813	0.843	0.828	0.853	0.841
Area (cm^2)	2.78	2.31	2.19	2.17	2.23	2.26
Force (N)	4448	4025	2469	3692	4381	2691
Strength (N/cm^2)	1598	1741	1130	1704	1962	1189

Table 14. Tensile Strength Results of Test Samples, Second Group, Seawater.

	Sample					
	1-J	1-K	2-J	2-K	3-J	3-K
Width (cm)	2.77	2.36	2.72	2.62	2.54	2.87
Thick. (cm)	0.942	0.876	0.853	0.810	0.828	0.831
Area (cm^2)	2.61	2.07	2.32	2.12	2.10	2.39
Force (N)	3936	4559	2491	4315	3025	3914
Strength (N/cm^2)	1509	2203	1074	2035	1438	1642
	4-J	4-K	5_J	5-K	6-J	6-K
Width (cm)	2.74	2.54	2.51	2.57	2.57	2.46
Thick. (cm)	0.831	0.851	0.871	0.828	0.826	0.833
Area (cm^2)	2.28	2.16	2.19	2.12	2.12	2.05
Force (N)	4092	3025	4092	2669	2291	4470
Strength (N/cm^2)	1796	1400	1868	1256	1082	2178

Table 15. Tensile Strength Results of Test Samples, Third Group, Fresh Water

	Sample					
	1-L	1-M	2-L	2-M	3-L	3-M
Width (cm)	3.07	2.54	2.51	2.64	257	2.46
Thick. (cm)	0.871	0.884	0.826	0.833	0.846	0.869
Area (cm^2)	2.68	2.25	2.08	2.20	2.17	2.14
Force (N)	2513	2913	4359	4626	2580	1512
Strength (N/cm^2)	938	1298	2100	2102	1189	707
	4-L	4-M	5-L	5-M	6-L	6-M
Width (cm)	2.72	2.92	2.87	2.72	2.59	2.62
Thick. (cm)	0.841	0.826	0.859	0.843	0.841	0.841
Area (cm^2)	2.28	2.41	2.46	2.30	2.18	2.20
Force (N)	4159	3158	2802	2313	2824	3914
Strength (N/cm^2)	1820	1310	1137	1003	1297	1780

Table 16. Tensile Strength Results of Test Samples, Third Group, Seawater.

	Sample					
	1-N	1-O	2-N	2-O	3-N	3-O
Width (cm)	2.51	2.67	2.64	2.54	2.95	3.12
Thick. (cm)	0.884	0.884	0.841	0.820	0.818	0.838
Area (cm^2)	2.23	2.35	2.22	2.08	2.41	2.62
Force (N)	4270	3514	2113	3047	3091	4492
Strength (N/cm^2)	1921	1491	952	1462	1283	1715
	4-N	4-O	5-N	5-O	6-N	6-O
Width (cm)	2.57	2.64	3.15	2.69	2.82	2.74
Thick. (cm)	0.851	0.864	0.886	0.826	0.902	0.864
Area (cm^2)	2.18	2.28	2.79	2.23	2.54	2.37
Force (N)	2513	3180	4404	3825	3803	3469
Strength (N/cm^2)	1151	1394	1578	1721	1496	1464

Table 17. Tensile Strength Results of Control Samples from the Laboratory and the Field Samples.

a) Control Samples

	Sample					
	1	2	3	4	5	6
Width (cm)	2.74	2.62	2.64	2.72	2.59	2.69
Thick. (cm)	0.853	0.810	0.884	0.828	0.856	0.871
Area (cm^2)	2.34	2.12	2.34	2.25	2.22	2.35
Force (N)	4159	3069	3403	4315	3714	2691
Strength (N/cm^2)	1776	1446	1457	1916	1673	1147

b) Field Samples

	Sample			
	1-Top	2-Top	3-Bottom	4-Bottom
Width (cm)	2.69	2.87	2.74	2.62
Thick. (cm)	0.739	0.798	0.721	0.744
Area (cm^2)	1.99	1.29	1.98	1.95
Force (N)	3825	3581	1890	1890
Strength (N/cm^2)	1922	1564	956	971

Mean Stress = 1569 N/cm^2

Table 18. Absorption and Specific Gravity of Asbestos Cement Specimens.

Sample	Weight, gms.			Results	
	Oven Dry	SSD	Saturated	Bulk Spec. Grav.	Absorption, (%)
1-D	42	51	26	1.68	21.4
2-D	32.5	39	20	1.71	20.0
3-D	47	57	28	1.62	21.3
4-D	35	42	21	1.67	20.0
5-D	33	40	20	1.65	21.2
6-D	35	42	21	1.67	20.0
1-E	43.5	52.5	26	1.64	20.7
2-E	47	57	28	1.62	21.3
3-E	46	56	28	1.64	21.7
4-E	35.5	43	21	1.61	21.1
5-E	38	46	23	1.65	21.1
6-E	47	56.5	28	1.65	20.2
1-F	38	46.5	24	1.69	22.0
2-F	33	38.5	19	1.59	24.0
3-F	31	38.5	19	1.59	24.0
4-F	39	47.5	24	1.66	22.0
5-F	30.5	37	18	1.61	21.3
6-F	33.5	42	21	1.60	25.0

Table 18 (continued)

Sample	Weight, gms.			Results	
	Oven Dry	SSD	Saturated	Bulk Spec. Grav.	Absorption, (%)
1-G	44.5	53.5	27	1.71	20.2
2-G	35	42.5	21	1.63	21.4
3-G	48	58.5	30	1.68	21.9
4-G	35.5	42	21	1.69	18.3
5-G	54	65	33	1.69	20.4
6-G	32.5	40	20	1.63	23.1
1-H	39	47	24	1.70	20.5
2-H	40	48.5	24	1.63	21.3
3-H	34	41.5	21	1.66	22.1
4-H	25	30.5	15	1.61	22.0
5-H	40.5	49.5	24	1.59	22.2
6-H	34	41.5	20	1.58	22.1
1-I	23.5	28	14	1.68	19.1
2-I	35	42	21	1.67	20.0
3-I	41	50	25	1.64	22.0
4-I	34	41.5	20	1.58	22.1
5-I	47	57	28	1.62	21.3
6-I	35.5	43	21	1.61	21.1

Table 18. (continued)

Sample	Weight, gms.			Results	
	Oven Dry	SSD	Saturated	Bulk Spec. Grav.	Absorption, (%)
1-J	35	42.5	22	1.71	21.4
2-J	33.5	40.5	21	1.72	20.9
3-J	40	48.5	25	1.70	21.3
4-J	39	47.5	24	1.66	21.8
5-J	41.5	50.5	26	1.69	21.7
6-J	42	51.5	26	1.65	21.4
1-K	42	51	26	1.68	21.4
2-K	42	51	26	1.68	21.4
3-K	34.5	42	21	1.64	21.7
4-K	41	50.5	25	1.61	23.8
5-K	53	64.5	33	1.68	21.7
6-K	43	52.5	27	1.69	22.1
1-L	27.5	34	17	1.62	23.6
2-L	44	53.5	26	1.60	21.6
3-L	32.5	39	20	1.71	20.0
4-L	37.5	45.5	22	1.60	21.3
5-L	36.5	45	22	1.59	23.3
6-L	34.5	42.5	21	1.60	23.2

Table 18. (continued)

Sample	Weight, gms.			Results	
	Oven Dry	SSD	Saturated	Bulk Spec. Grav.	Absorption, (%)
1-M	37	45	22	1.61	21.6
2-M	35	42	21	1.67	20.0
3-M	39	48	23	1.56	23.1
4-M	34	41.5	20	1.58	22.1
5-M	33	40	20	1.65	21.2
6-M	34	42	21	1.62	23.5
1-N	38.5	47	24	1.67	22.1
2-N	44	53	27	1.69	20.5
3-N	35.5	43.5	22	1.65	23.0
4-N	40.5	49	24	1.62	21.0
5-N	32.5	39.5	20	1.67	21.5
6-N	45	56	28	1.61	24.4
1-O	53	64.5	33	1.68	21.7
2-O	42	50.5	26	1.71	21.3
3-O	26	32	16	1.63	23.1
4-O	38.5	47	24	1.67	22.1
5-O	37.5	46	23	1.63	22.7
6-O	55.5	67.5	34	1.66	22.5

Table 18. (continued)

Sample	Weight, gms.			Results	
	Oven Dry	SSD	Saturated	Bulk Spec. Grav.	Absorption, (%)
1	55	67	33	1.62	21.8
2	36.5	44	22	1.66	21.0
3	43.5	52.5	26	1.64	20.7
4	45	54.5	27	1.64	21.1
5	34	41	20	1.62	20.6
6	35	43	21	1.59	20.0
1-Top	41.5	50.5	25	1.63	21.7
2-Top	56	70	33	1.51	25.0
3-Bottom	33	50.5	19	1.05	53.0
4-Bottom	26	39.5	15	1.06	51.9

Appendix B.

Calculations of the Number of Samples Needed for the Wetting/Drying Test Program

$$n = \frac{t_{\alpha}^{2}\,\sigma^{2}}{\Delta^{2}},$$

Where, n = the # of samples,
t = a statistical parameter,
σ = the standard deviation of the maximum stress values,
Δ = the confidence interval,
υ = (# of pilot test samples) - 1,
and α = the area under the distribution curve.

1) Control Samples

Level of confidence = 95%

$\alpha/2 = 0.025$

$\nu = 9 - 1 = 8$

$t_{\alpha/2} = 2.306$

$\sigma = 128.74\ N/cm^2$

$\Delta = 190\ N/cm^2$

$$n = \left[\frac{2,306\ (128.74)}{190}\right]^2 = 3$$

2) Wet and Dried Samples

Level of confidence = 95%

$\alpha/2 = 0.025$

$\upsilon = 10 - 1 = 9$

$t_{\alpha/2} = 2.262$

$\sigma = 292.64\ N/cm^2$

$\Delta = 190\ N/cm^2$

$$n = \left[\frac{2.262\ (292.64)}{190}\right]^2 = 12$$